

People's Democratic Republic of Algeria
Ministry of Higher Education and Scientific Research
University M'Hamed BOUGARA – Boumerdes



Institute of Electrical and Electronic Engineering
Department of Electronics

Final Year Project Report Presented in Partial Fulfilment of
the Requirements for the Degree of

MASTER

In Electronics

Option: Computer Engineering

Title:

**Design and implementation of an
automatic sun tracker system**

Presented by:

- **MERAINI Abdelaaziz**

Supervisor:

Dr. BELAIDI Dehia

Registration Number:...../2019

All praise is due to Allah the merciful and the beneficent.

I would like to express my special thanks of gratitude to my supervisor Dr Belaidi Dehia as well as Mr chibani A.malek & Dr A.DJALIL Dahbi from Research Unit of Renewable Energies (URERMS/ADRAR) who gave me the golden opportunity to do this wonderful project on the topic of Implementation and Design of dual axis solar tracking system, which also helped me in doing a lot of Research and I came to know about so many new things I am really thankful to them.

I would also like to thank my family and friends who helped me a lot in finalizing this project within the limited time frame.

DEDICATION

Every challenging work needs self-efforts as well as guidance of elders especially those who were very close to me. My humble efforts is dedicated to my family and friends: to extraordinary mother, without her I would never reached this level of education.

To my dear brother, he always encouraged me and believed in me even when I didn't believe in myself.

Thanking my parents is the least thing that I can do. Their care, love and support encouraged me to continue until the end.

A special dedication to a special person "ISLAM", I am really grateful to have him in my life. He believed in my capability of reaching to this point throw-out the last years and I thank him for his unlimited helps, and for his advices. I give the great appreciations for his encouraging words.

To all my family and my precious friends, especially BILEL TOUZOUT, YUCEF, RAFIK, REDOUANE HOUSSEYN and WALID with whom the bad moments of these years have been sweet, and the good ones unforgettable.

To all relatives, friends and others who in one way or another shared their supports, either morally, financially and physically.

ACKNOWLEDGEMENTS

TABLE OF CONTENTS

LIST OF FIGURES AND TABLES

ABSTRACT

GENERAL INTRODUCTION.....1

CHAPTER ONE: Generalities on Solar Energy

Introduction.....2

1. Status and Prospects of PV Technology.....2
2. Solar Power Fundamentals.....4
 - 2.1. Sun Radiation.....4
 - 2.2. Daily insolation latitude and season change.....5
 - 2.3. The Working Principle of Solar Cells.....5

CHAPTER TWO: Methods to Increase Efficiency

- 2.1 Preamble.....7
- 2.2 First method Implementation of MPP Tracker.....7
 - 2.2.1 MPPT Algorithms.....8
 - 2.2.2 Problem of MPPT in case of partial shading.....8
- 2.3 The second method Using Solar Tracking Mechanisms9
 - 2.3.1 Types of Trackers.....10
 - 2.3.2 Single Versus dual axis trackers.....10
 - 2.3.3 Advantages and Drawbacks of Different Trackers.....13
 - 2.3.3.1 Advantages and drawbacks of open loop Tracker.....13
 - 2.3.3.2 Advantages and drawbacks of closed loop Tracker.....14

CHAPTER THREE: Simulation of the system

- 3.1 introduction.....15
- 3.2 the components implanted in the simulation.....15
 - 3.2.1 Proteus.....15
 - 3.2.2 The Sensor device.....16
 - 3.2.3 Microcontroller (Arduino Mega 2560)17
 - 3.2.4 The Servo motor.....18
 - 3.2.5 The whole schematic diagram of the simulated system.....19
- 3.3 The flow code.....21
- 3.4 The simulation results22

CHAPTER four: implementation of the system.

- 4.1 Introduction24
- 4.2 The tracker design and choice of components24
 - 4.2.1 The Sensor device.....24
 - 4.2.2 The Servomotor.....26
 - 4.2.3 Arduino MEGA 2560.....29
 - 4.2.4 The Data logger module (The SD card module.....30
 - 4.2.5 The Current sensor module ACS71231
 - 4.2.6 The voltage sensor module32

4.2.7	DS1307 RTC module.....	33
4.2.8	Solar cell	33
4.3	Software inmplementation.....	34
4.4	The assembling of the whole system of tracking	36
4.5	Experimental results and data analysis.....	38
4.5.1	Mobile versus static pv depending on light direction.....	38
4.5.2	Data analysis.....	39
Conclusion		
Appendix		
References		

List of figures and tables

CHAPTER ONE: Generalities on Solar tracker

Fig 1-1: Local solar irradiance averaged over three years from 1991 to 1994 (24 hours a day), taking into account the cloud coverage available from weather satellites	2
Fig 1-2: Installed power capacity of Solar PV in the world	3
Fig 1-3: (a) Development of the installed capacity (in GW) of several electricity generation technologies since 1980. (b) The same Graph corrected by the capacity factor Cf and extrapolated until 2020.....	3
Fig 1-4: Daily insolation for horizontal plane	5
Fig 1-5: a very simple solar cell model.....	6
Fig 1-6: The incident angle formed between the normal to cell and sunlight circuit, they will recombine with holes.....	6

CHAPTER TWO: Methods to Increase Efficiency

Fig 2-1: Effect of Temperature on the Solar Cell performance.....	7
Fig 2-2: Effect of the Irradiance on the Solar Cell Performance.....	8
Table 2-3: Comparison of Different MPPT techniques.....	8
Fig 2-4: Classification of Solar Trackers.....	12
Fig 2-5: Instruments of measuring irradiance.....	13

CHAPTER THREE: Simulation of the System

Fig 3-1: Front page of proteus.....	16
Fig 3-2a: the sensor	16
Fig 3-2b: the LDRs	17
Fig 3-3: the Arduino mega.....	18
Fig 3-4: the servomotor.....	19
Fig 3-5: The whole circuit built by proteus.....	20
Fig 3-6: Flowchart of the simulated system	21
Fig 3-7: Results of the simulation.....	22

CHAPTER FOUR: Implementation of the System

Fig 4-1: LDR resistor connection as voltage divider.....	24
Fig4-2: Photoresistor” Light Dependent Resistor”	25
Fig 4-3: Arrangement of LDR sensors for a single axis follower.....	26
Fig 4-4: Servomotor SG90.....	27
Fig 4-5: Servomotor pinout.....	27
Fig 4-6: Angular displacement of a servomotor.....	28
Fig 4-7: The card Arduino MEGA2560.....	29
Fig 4-8: Arduino Mega card features.....	29
Table 4-1: Arduino card features	30
Fig 4-9: The SD Card module.....	31
Table 4-2: Interfacing the SD Card module to the arduino.....	31
Fig 4-10: The Current sensor module.....	31
Fig 4-11: The voltage sensor module.....	32
Fig 4-12: The real time clock Module.....	33
Fig 4-13: The solar cell.....	33
Fig 4-14: The flowchart of the system.....	35
Fig 4-15: The dual axis tracker.....	37
Fig 4-16: The tracker after operating.....	38
Table4-3: Variation of the output of the static cell VS time	39
Table 4-4: Variation of the output of the cell on tracker VS time.....	39
Fig 4-17: The comparison of power curves for both the static and tracking panel....	40

Abstract

Renewable energy solutions are becoming increasingly popular. Photovoltaic (solar) systems are but one example. Maximizing power output from a solar system is desirable to increase efficiency. In order to maximize power output from solar panels, one needs to keep the panels aligned with the sun. As such, a means of tracking the sun is required.

This is definitely a more cost effective solution than purchasing additional solar panels. It has been estimated that the yield from solar panels can be increased by 30 to 60 percent by utilizing a tracking system instead of a stationary array. This study evaluates the performance of two photovoltaic systems: one fixed and one equipped with a sun tracker which is a prototype for a microcontroller-based multi-function solar tracking system.

The analysis accounts also the energy consumption of the sun tracker. An analytical approach is proposed. To validate the results through experimental tests, two alternative low power PV systems were built.

***Keywords—solar tracking; single axis; dual axis; light
depending resistor (LDR), Data acquisition, servo motor, Arduino.***

Introduction

Solar energy is the energy extracted from the rays issued from the sun in the form of heat and electricity. This energy is essential for all life on Earth. It is a renewable resource that is clean, economical, and less pollution compared to other resources and energy [1]. Therefore, solar energy is rapidly gaining notoriety as an important means of expanding renewable energy resources. As such, it is vital that those in engineering fields understand the technologies associated with this area. Our report includes the design and implementation of a microcontroller-based solar tracking system. Solar tracking allows more energy to be produced because the solar panel is tracking the maximum power point of the sun's position.

Nowadays, the popularity of solar energy and electricity combined with the reduced cost per peak watt are having a direct effect on increasing residential solar power system. But it is still very expensive compared to what the electric utility company charges per kilowatt hour [2]. In addition, large solar panels need a perfect fixed installation to get maximum sun light and consume much power to turn left or right around a single axis every hour or so.

To get an efficient solar tracker system, a small solar panel is used instead of a large one to obtain a graphical position data of the sun when it is detected and send this data to the large panels. This system can be installed anywhere in the world without knowing the sun directions and seasons.

In order to develop our work, we organized the manuscript as follow:

The first chapter presents generalities on solar energy.

The second exhibits the different solution to increase efficiency of solar cell.

The third one is dedicated to the simulation part of this work.

The fourth one referred to the implementation of the automatic tracker system.

chapter /

Generalities on Solar Energy

Introduction

Before discussing the solar tracking systems, we'll review some fundamental solar radiation concepts and mention some significant values to better comprehend the outcomes of this job.

1.1. Status and Prospects of PV Technology

“Solar energy”, as previously stated, refers to the radiation energy of the sun that can be converted into power with special devices. Figure 1-1 shows the irradiance levels around the world, since the available amount of solar energy differs dramatically. The devices can be classified according to the technology used or how the energy is applied, for example, to generate electricity or for solar thermal heating.

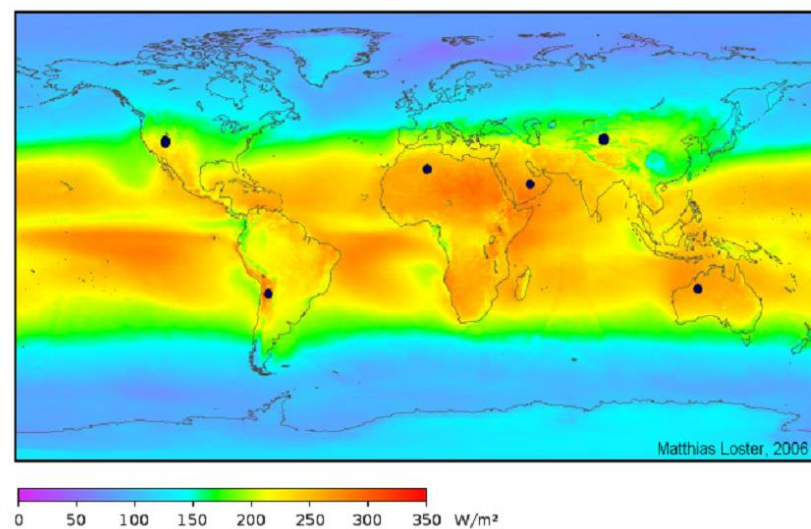


Fig 1-1: Local solar irradiance averaged over three years from 1991 to 1994 (24 hours a day), taking into account the cloud coverage available from weather satellite[3].

The solar thermal energy is mostly used to heat up water or air, using solar thermal panels for domestic hot water or space heating. Under the electricity generating group, the concentrating plants and the photovoltaic (PV) panels are the most known. While the first are used on larger fields in the form of power plants to generate power connected to the grid, the second are not necessary used in larger power plants but also in smaller systems for domestic use, either as grid-tied or off-grid PV systems. An approximation of the installed capacity of global PV systems can be seen in Figure 1-2. The tendency shows that grid-connected systems are becoming much more important than off-grid systems, while the growing tendency has increased significantly. The estimated grid-connected solar PV installed capacity in the year 2018 worldwide was 508 GW. China, the country with the largest installed capacity, had 48.32 GW (REN21, 2018). Between 2017 and 2047 the renewable power generation capacity saw its largest annual increase ever with an estimated 178 gigawatts [4].

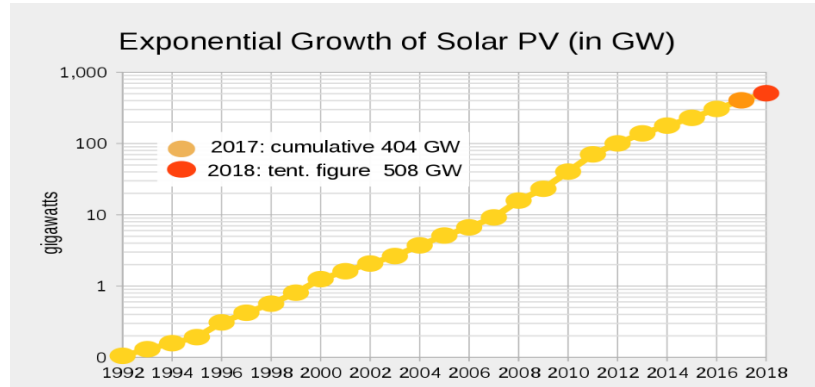


Fig 1-2: Installed power capacity of Solar PV in the world. [5].

Solar power plants either connected or not to the grid, have a similar component configuration. For the grid connected ones, the power plants consist mainly of solar modules, the inverter, the data logger, some sensors, a grid supply meter, the mounting parts and other components that could be used. Basically, the solar modules collect the solar radiation and generate DC current which is transformed into AC current by the inverter and then delivered to the grid. For the solar modules, there are many cell types whose efficiency vary significantly, such as single-crystalline silicon ($\eta = 14\%$ to 18%), polycrystalline ($\eta = 13\%$ to 15.5%), thin films ($\eta = 10\%$ to 12%) and amorphous silicon ($\eta = 6\%$ to 8%).

Figure 1-3 shows the effective installed power corrected with the capacity factors. Currently solar energy generates about an order of magnitude less electricity than wind energy and more than two orders of magnitude less than hydro and nuclear electricity.

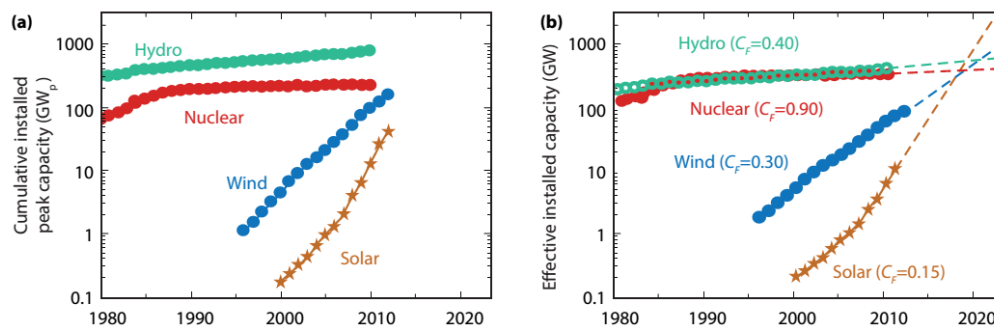


Fig 1-3 (a) Development of the installed capacity (in GW) of several electricity generation technologies since 1980. (b) The same Graph corrected by the capacity factor C_f and extrapolated until 2020.

Seen the development in recent years we, however, can claim that the trend in the growth of solar energy will continue the coming years. If we therefore extrapolate the trends of the last decade until 2020 we see that the installed power of solar energy will exceed nuclear, wind and hydropower by then. It is just a matter of time until solar electricity

will be the most important electricity generation technology that is not based on combustion of fossil fuels [6].

There are a series of possibilities for connecting the solar modules to the inverter (in series, in parallel or in combination) and which additional parts should be used, mostly for measurement purposes. However, these connecting options are mostly related with the inverters' characteristics or on how many solar modules are being used. To increase the collected amount of energy, considering a determined amount of solar panels, one of the options is to enhance the panels orientation. This can be achieved by installing fixed systems at an optimal orientation angle or by using tracking systems which follow the sun.

1.2 Solar Power Fundamentals

1.2.1 Sun Radiation

The sun has an effective blackbody temperature of 5777K, radiation emitted by the sun reaches the earth's surface at a maximum flux density of 1kW/m^2 as a short wave radiation. Depending on the time, place and weather the energy flux can vary from 3MJ/m^2 to 30MJ/m^2 in a single day. This energy is a very high energy and can be used for thermally, photophysical or photochemical processes. The emitted radiation reaches the earth atmosphere at almost fixed intensity at a solar constant of 1367W/m^2 [7]. This number varies with the variation of the earth-sun distance and therefore it is dependent with the time of the year. Figure 1-4 shows the variation of these radiation during different seasons in one year. Beneath the atmosphere, the solar radiation will enter the earth surface as extraterrestrial beam radiation and it will varies widely due to local atmospheric variations, location (latitude), time of the day and season of the year. After entering the earth's atmosphere, the extraterrestrial beams will part to beam radiation that received without having being scattered by the atmosphere and diffuse radiation that received after its direction has been changed by scattering with the atmosphere. And the sum of both radiations called the global radiation. However, the amount of these radiation depends on the sky condition and therefore the portion of these radiation varies but there is always be at least 10% of diffuse radiation, this is because the effect of the particles and molecules radiation's absorption in the atmosphere.

1.2.2 Daily insolation, latitude and season change

A good term that can be used to easy compare the amount of energy received by a surface in a single day is the daily insolation. The amount of daily insolation varies with the season of the year and the location. Figure below shows how this can changes with change of the latitude and the season of the year for a horizontal surface. The greater the latitude the less insolation can be received especially in winter.

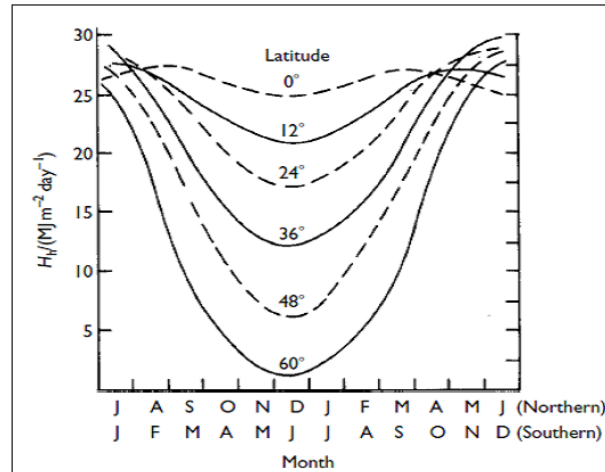
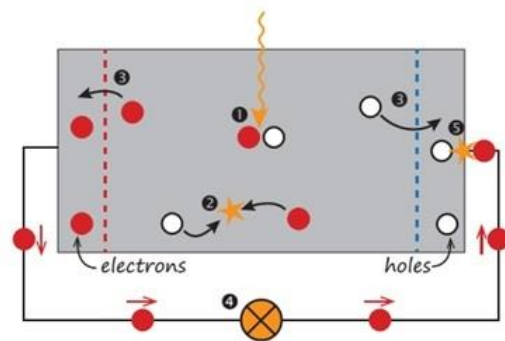


Fig 1-4 Daily insolation for a horizontal plane change with season and latitude.

1.3 The Working Principle of Solar Cells

A fundamental understanding of how a photovoltaic panel works is essential in producing a highly efficient solar system. Solar panels are formed out of solar cells that are connected in parallel or series. When connected in series, there is an increase in the overall voltage, connected in parallel increases the overall current. Each individual solar cell is typically made out of crystalline silicon, although other types such as ribbon and thin-film silicon are gaining popularity. PV cells consist of layered silicon that is doped with different elements to form a p-n junction. The p-type side will contain extra holes or positive charges. The n-type side will contain extra electrons or negative charges. This difference of charge forms a region that is charge neutral and acts as a sort of barrier. When the p-n junction is exposed to light, photons with the correct frequency will form an extra electron/hole pair. However, since the p-n junction creates a potential difference, the electrons can't jump to the other side only the holes can. Thus, the electrons must exit through the metal connector and flow through the load, to the connector on the other side of the junction.

Fig 1-5: A very simple solar cell model. **1** Absorption of a photon leads to the generation of an electron-hole pair. **2** Usually, the electrons and holes will combine. **3** With semi-permeable membranes the electrons and the holes can be separated. **4** The separated electrons can be used to drive an electric circuit. **5** After the electrons passed through the circuit, they will recombine with holes.



Since the PV cells generate a current, cells/panels can be modeled as DC current sources. The amount of current a PV panel produces has a direct correlation with the intensity of light the panel is absorbing. Below is a simple drawing of the system:

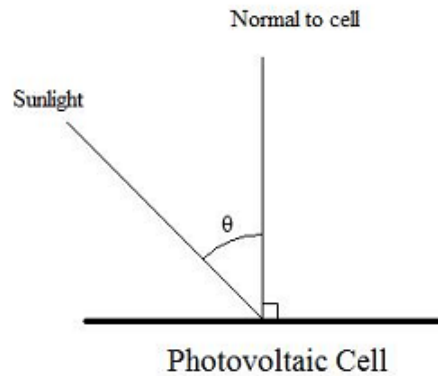


Fig 1-6: The incident angle formed between the normal to cell and sunlight

The normal to the cell is perpendicular to the cell's exposed face. The sunlight comes in and strikes the panel at an angle. The angle of the sunlight to the normal is the angle of incidence (θ). Assuming the sunlight is staying at a constant intensity (λ) the available sunlight to the solar cell for power generation (W) can be calculated as:

$$W = A \lambda \cos(\theta)$$

Here, A represents some limiting conversion factor in the design of the panel because they cannot convert 100% of the sunlight absorbed into electrical energy. By this calculation, the maximum power generated will be when the sunlight is hitting the PV cell along its normal and no power will be generated when the sunlight is perpendicular to the normal. With a fixed solar panel, there is significant power lost during the day because the panel is not kept perpendicular to the sun's rays. A tracking system can keep the angle of incidence within a certain margin and would be able to maximize the power generated. Mousazadeh et al. calculated the amount of power gained by tracking can come close to an ideal 57% difference [8].

chapter I/

Methods of increasing efficiency

2.1 Preambles.

There exist many cell types for the solar modules whose efficiency vary significantly, such as single-crystalline silicon ($\eta = 14\%$ to 18%), polycrystalline ($\eta = 13\%$ to 15.5%), thin films ($\eta = 10\%$ to 12%) and amorphous silicon ($\eta = 6\%$ to 8%).

Due to the poor conversion efficiency and to the I-V characteristics of the solar cells, a considerable part of this converted amount is wasted. In order to improve the overall gain, experts either:

- Implement an electronic circuit for MPPT (Maximum Power Point Tracking).
- Make the Solar Tracking System.
- Use the two techniques to harvest the maximum energy; although, the hybrid solution seems to be the best solution, it is relatively complex and not cost effective one.

2.2 The 1st Method: Implementation of MPP Tracker

PV array has an optimum operating point to extract the maximum power called the maximum power point (MPP), which varies depending on cell temperature and irradiance level, as shown in Fig. 2-1 and Fig. 2-2 respectively. Variation in lighting intensity causes these trackers to deviate from the maximum power point when lighting conditions change, the tracker needs to response within a short time to the change to avoid energy loss. Therefore, it is not easy to track the maximum power point of the PV cell quickly and effectively in the real application.

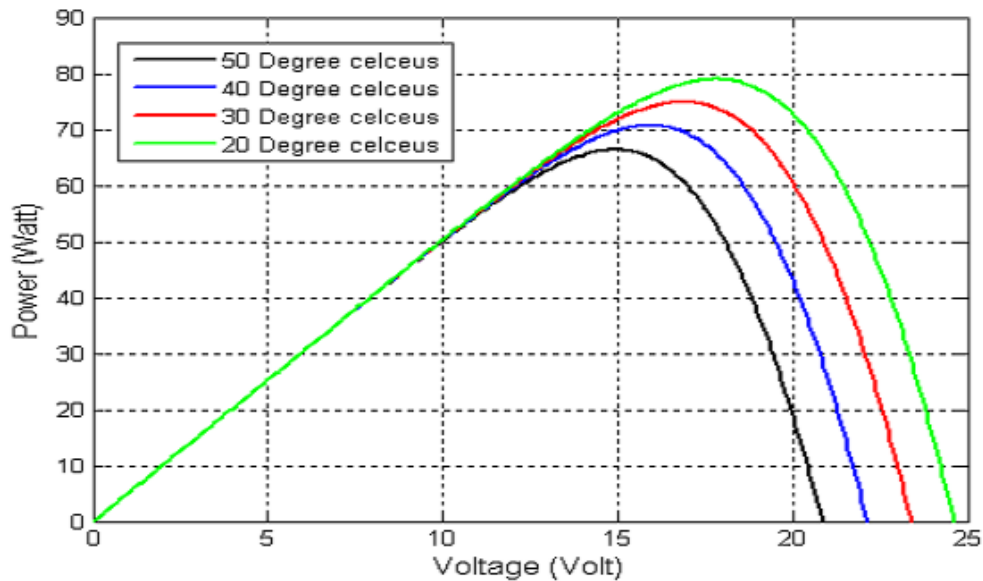


Fig 2-1 Effect of Temperature on the Solar Cell performance [9]

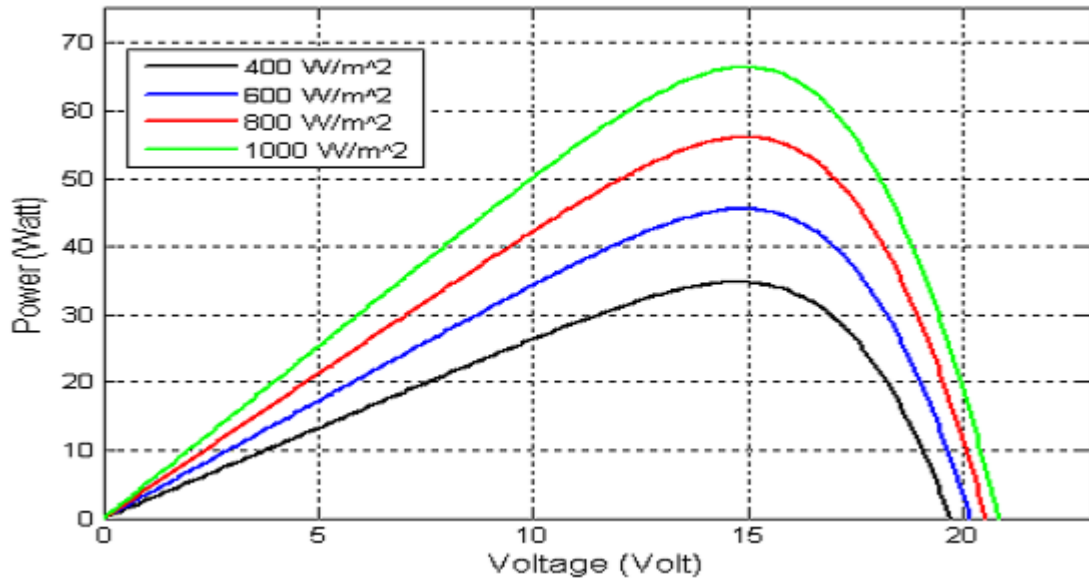


Figure 2-2: Effect of the Irradiance on the Solar Cell Performance [9]

2.2.1 MPPT Algorithms

There are several MPPT Algorithms (see appendix), each one having advantages and drawbacks, since MPPT Algorithms is outside the scope of our work, we will give a table that compare the different algorithms used and their features:

MPPT TECHNIQUE	SPEED	COMPLEXITY	RELIABILITY	IMPLEMENTATION
Fractional Short Circuit current	Medium	Medium	Low	Digital/Analog
Fractional Open Circuit voltage	Medium	Low	Low	Digital/Analog
Incremental Conductance	Varies	Medium	Medium	Digital
Hill Climbing	Varies	Low	Medium	Digital/Analog
Fuzzy logic	Fast	High	Medium	Digital
Neural Network	Fast	High	Medium	Digital

Table 2.3: comparison of Different MPPT techniques

2.2.2 Problem of MPPT

The main problem solved by the MPPT algorithms is to automatically find the panel operating voltage that allows maximum power output. In a larger system, connecting a single MPPT controller to multiple panels will yield good results [10] but, in the case of partial shading, the combined power output graph will have multiple peaks and valleys (local maxima). This will confuse most MPPT algorithms and make them track incorrectly. Some techniques to solve problems related to partial shading have been proposed, but they either need to use additional equipment (like extra monitoring cells, extra switches and current sensors for sweeping panel current), or complicated models based on the panel characteristics (panel array dependent). These techniques only make sense in large solar panel installations, and are not within the scope of this application note.

Ideally, each panel or small cluster of panels should have their own MPPT controller. This way the risk of partial shading is minimized, each panel is allowed to function at peak efficiency, and the design problems related to converters handling more than 20-30A are eliminated [11].

2.3 The 2nd Method: Using Solar Tracking Mechanisms

Solar tracking can be implemented by using one-axis [12], and for higher accuracy, two-axis sun-tracking systems [13-14]. For a two-axis sun-tracking system, two types are known as: polar (equatorial) tracking and azimuth/elevation (altitude–azimuth) tracking. The solar tracker, a device that keeps PV or photo-thermal panels in an optimum position perpendicular to the solar radiation during daylight hours, increases the collected energy. The first tracker introduced by Finster in 1962, was completely mechanical. One year later, Saavedra presented a mechanism with an automatic electronic control, which was used to orient an Eppley pyrhelimeter.

Trackers **need not** point directly at the sun to be effective. If the aim is off by 10 degrees, the output is still 98.5% of that of the full-tracking maximum.

In the cloudiest, haziest locations the gain in annual output from trackers can be in the low 20% range. In a generally good area, annual gains between 30 and 40% are typical. The gain in any given day may vary from almost zero to nearly 100%.

2.3.1 Types of Trackers

There are two types of solar tracking systems: **single-axis** and **dual-axis**.

- A **single-axis tracker** moves your panels on one axis of movement, usually aligned with north and south. These setups allow your panels to arc from east to west and track the sun as it rises and sets.
- A **dual-axis tracker** allows your panels to move on two axes, aligned both north-south and an east-west. This type of system is designed to maximize your solar energy collection throughout the year. It can track seasonal variations in the height of the sun in addition to normal daily motion, this tracking system include closed and open loop control mechanisms. The PV panels are positioned by the help of photo sensors and feedback controllers. The open loop one is based on calculations of the seasonal weather and the sun position. The hybrid control is made up of both closed and open loop tracking systems. The performance of the electro-optical tracking systems such as sun sensor composed of four photo resistors with cylindrical shades is better depending on good weather conditions. This adjustment can be realized more easily with two axes sun tracking systems than single ones which is cheaper and simpler to design [15].

2.3.2 Single Versus Dual axis trackers

If a tracking system is not used, the solar panel should still be oriented in the optimum position. The panel needs to be placed where no shadow will fall on it at any time of the day. Additionally, the best tilt angle should be determined based on the geographical location of the panel. As a general guideline for the northern hemisphere, the PV panel should be placed at a tilt angle equal to the latitude of the site and facing south [16]. However, for a more accurate position and tilt angel a theoretical model of the suns iridescence for the duration of a year is created and the angel and position is matched to the model. Using one axis of tracking can provide a significant power gain to the system. Wikipedia claims that one axis trackers are placed into the following classifications: horizontal single axis tracker (HSAT), vertical single axis tracker (VSAT), tilted single axis tracker (TSAT), and polar aligned single axis tracker (PASAT). However, these terms don't seem to be used in most articles discussing tracking methods. One article did mention that a TSAT at a tilt angle of 5° increases the annual collection radiation by 10% compared to a HSAT, a HSAT increases the annual collection radiation by 15% to a VSAT, and finally a PASAT increases the annual

collection radiation by 10% over a HSAT [17]. Thus for one axis a PASAT or TSAT configuration would collect the most solar radiation.

The percent gain from going from a PSAT to a dual-axis system is small [18], but as long as the system doesn't use more power than gained, it still helps. Again Wikipedia mentions two classifications for dual axis trackers: Tip-Tilt Dual Axis Tracker (TTDAT) and Azimuth Altitude Dual Axis Tracker (AADAT). The difference between the two types is the orientation of the primary axis in relation to the ground. TTDAT's have the primary axis horizontal to the ground and AADAT's have theirs vertical. The azimuth/altitude method seems to be largely used, based on its reference in multiple research articles on tracking. In the article by Sefa et al. the following was stated; "The results indicated that increases of electrical power gains up to 43.87% for the two axes, 37.53% for the east– west, 34.43% for the vertical and 15.69% for the north–south tracking, as compared with the fixed surface inclined 32 to the south in Amman" [19].

As we can see in figure 2-4 a classification of all sun trackers reviewed in a diagram.

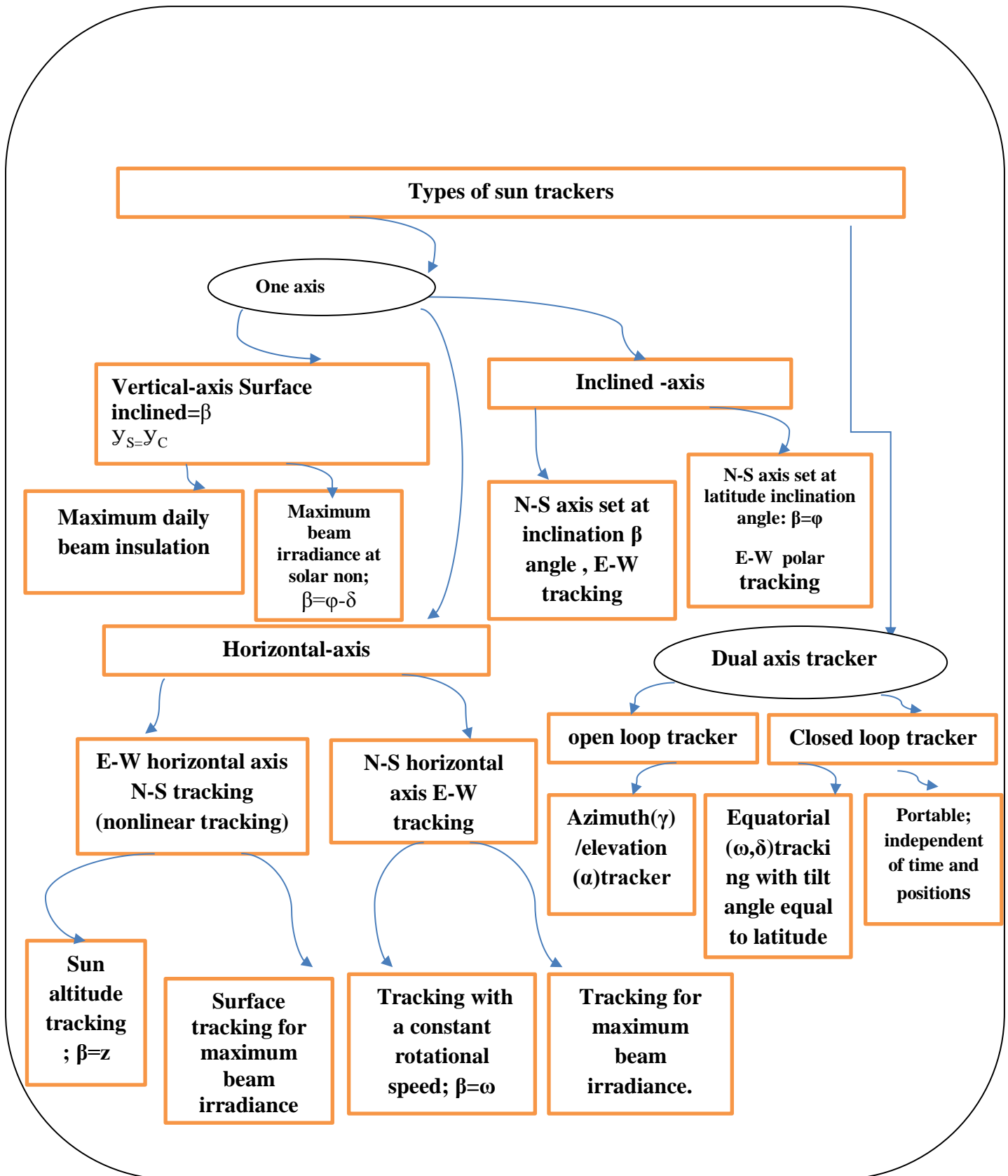


Figure 2-4 Classification of Solar Trackers.

2.3.3 Advantages and Drawbacks of Different dual axis Trackers

In the following section, different types of dual axis trackers are viewed in terms of their advantages and drawbacks.

2.3.3.1 Advantages and drawbacks of open loop Tracker

An open loop system will operate according to a Sun Position Algorithm and for most of the developed algorithms at the present time, they are complex and therefore they have a long runtime which will make the microcontroller and motors of the tracker consume a significant amount of energy, those complex and long algorithms like the one developed by National Renewable Energy Laboratory (NREL), Are used to calibrate Solar radiation measurement equipment like The pyrhelimeter shown in figure 2-5a which is used for measurement of direct solar irradiance, for this reason, it is mounted on a high accuracy solar tracking mechanism. Sunlight enters the instrument through a window and is directed onto a thermopile which converts heat to an electrical signal that can be recorded. The signal voltage is converted via a formula to measure watts per square meter.

Also we can mention Pyranometer listed in figure 2-5b which is also mounted on a very accurate solar tracker and it is used to measure the diffused irradiance (The light beam coming from all surrounding objects excluding the light coming from the sun).

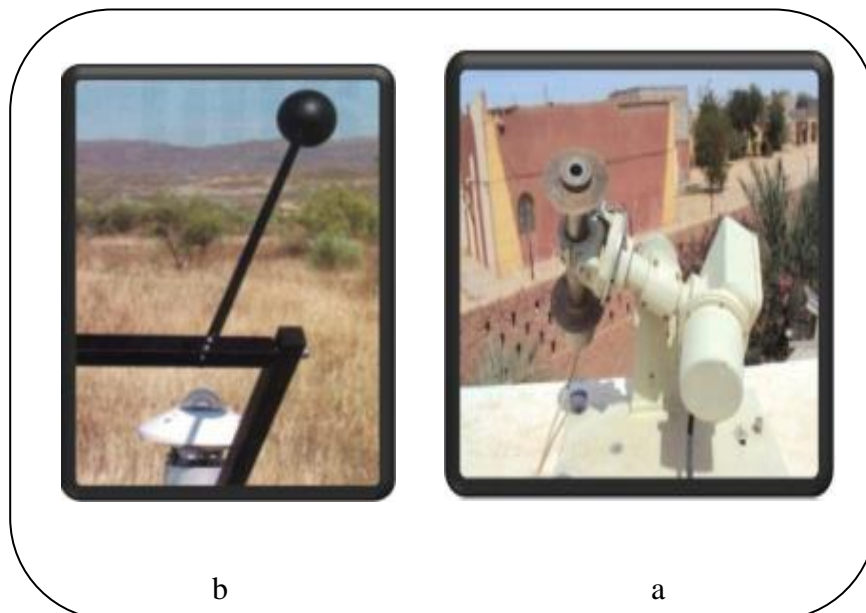


Figure 2-5 : instruments of measuring irradiance

The other type of algorithms which give the position of sun is relatively simple and do not require considerable time to output the calculated angle thus less energy consumption, but the speed of execution will come at the expense of accuracy, the tracker will diverge from the desired position due to the accumulated errors.

Most of these simple algorithms are valid only for specific regions and for a certain number of years.

In addition to its significant consumption of energy, this type of trackers requires a GPS module which is quite expensive.

2.3.3.2 Advantages and drawbacks of closed loop Tracker:

A closed loop system is equipped with 4 Light Dependent Resistors (LDR) working as Light sensors, by using a microcontroller, motors will rotate in the direction of the LDR that receives the highest amount of light.

According to experiments conducted in Bouzarea and ghardaia [20], it was shown that Dual Axis Solar Tracking System will outperform the fixed System ONLY if the weather is Sunny which means the system spends more energy than the generated one in the of quick weather changes ,having said this however, since the tracker will be implemented on regions that has plenty of sun, the output of closed loop Tracker is better than that of the fixed solar panels.

chapter III

Simulation of The system



3.1. Introduction

In our design, the aim of this simulation is to design and simulate a sun tracker which is able to keep the solar photovoltaic cell perpendicular to the sun throughout all the time in order to make it more efficient. The dual axis solar photovoltaic cell acquires data from the LDRs immediately and the tracking system has the capability to always point the solar array toward the sun and can be installed in various areas with no modifications. The vertical and horizontal motion of the panel is obtained by using two servomotors. The microcontroller (Arduino) has been used to control the position of the motors. The received data from the sensors control of dual axis solar tracking system and ensures the point to point motion of the servomotors while tracking the sun.

3.2. The components implanted in the simulation

We will separately quote each component alone and make a screenshot of that element independently to the whole system.

3.2.1 Proteus

We used proteus as a simulation software which is made for microprocessor simulation, schematic capture, and printed circuit board (PCB) design, it is developed by Labcenter Electronics. The XGameStation Micro Edition was designed using Lab center's. Proteus schematic entry and PCB layout tools. Proteus PCB design combines the ISIS schematic capture and ARES PCB layout programs to provide a powerful, integrated and easy to use suite of tools for professional PCB Design. All Proteus PCB design products include an integrated shape based auto router and a basic SPICE simulation capability as standard. More advanced routing modes are included in Proteus PCB Design Level 2 and higher whilst simulation capabilities can be enhanced by purchasing the advanced simulation option and/or micro-controller simulation capabilities, and here in figure 3-1 we can see the interface of that software.

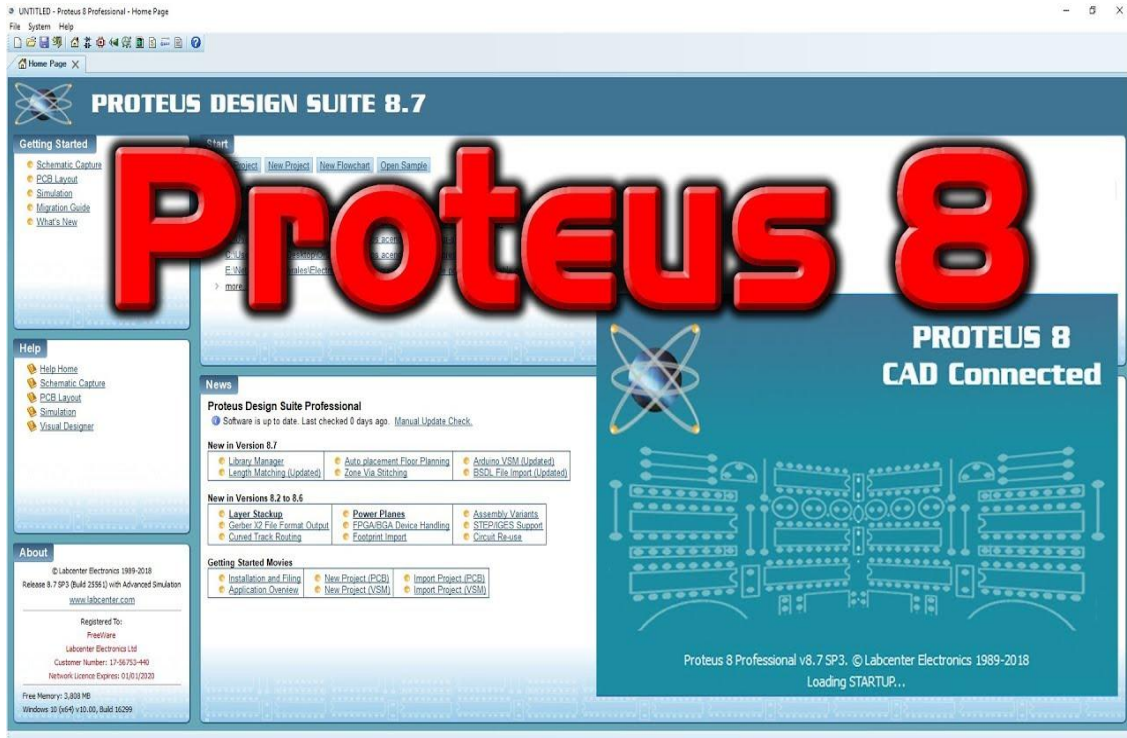


Figure 3-1: Front page of Proteus

3.2.2 The Sensor device

We assembled a sensor device by composing a four parallel of a light dependent resistor (LDR) made in series with a 10k resistor, this arrangement is based on a voltage divider; in order to get the voltage between each resistor of the four which is connected to the inputs of the controller device and all that configuration employed to implement that algorithm and the following figure 3-2a shows whole circuit of the sensor.

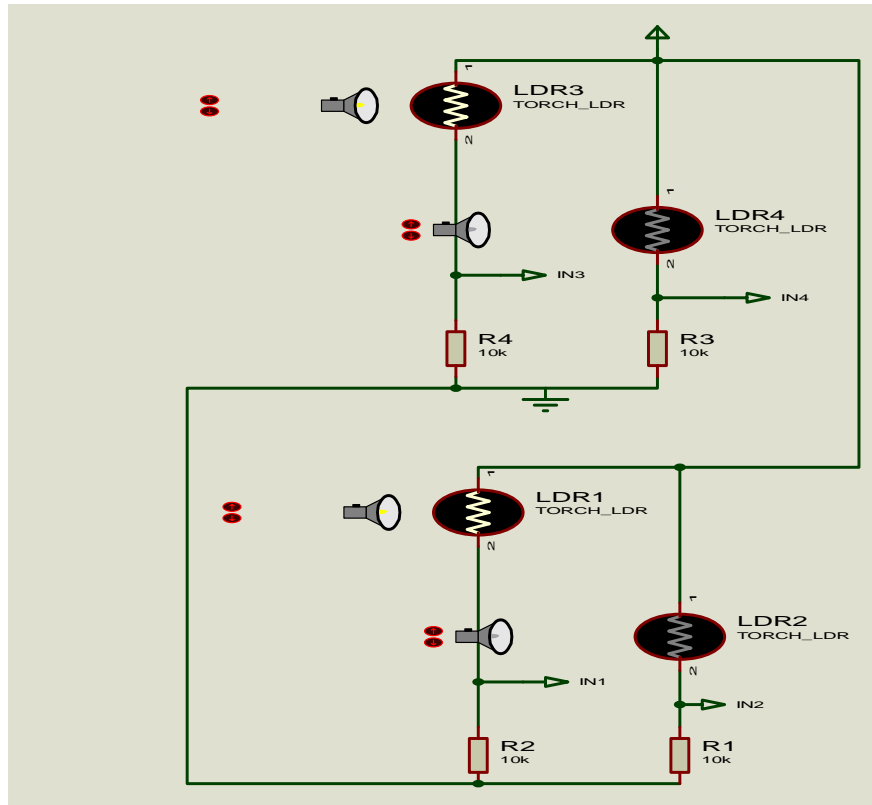


Figure 3-2a: circuit of the sensor by Proteus

Let's talk about the light dependent resistor, this component is a dipole that decreases its resistance when illuminated. Placed in a closed circuit, it modifies the intensity of the current under the action of light, softwarely we adjust the intensity of light by using the + and – situated in front of the LDR, the figure 3-2b display this last.

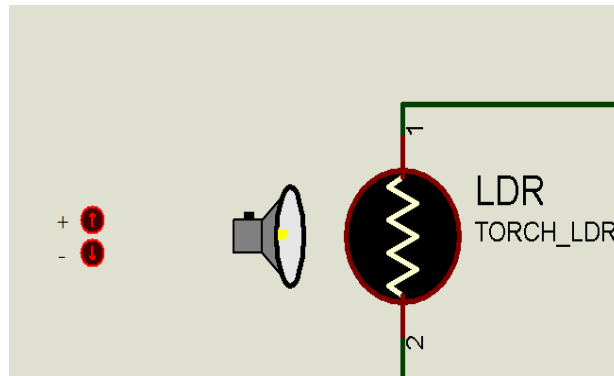


Figure 3-2b: the LDRs

3.2.3 The Microcontroller (Arduino mega 2560)

We control this system by the Arduino mega 2560 which is a microcontroller board based on the ATmega2560, it consists of digital input/output pins, and analog inputs, and a reset button. It contains everything needed to support the microcontroller. It controls the desired system by uploading the file of the program which can be done in

C language. And it's figured in the following figure 3-3 which represent a screenshot of that element.

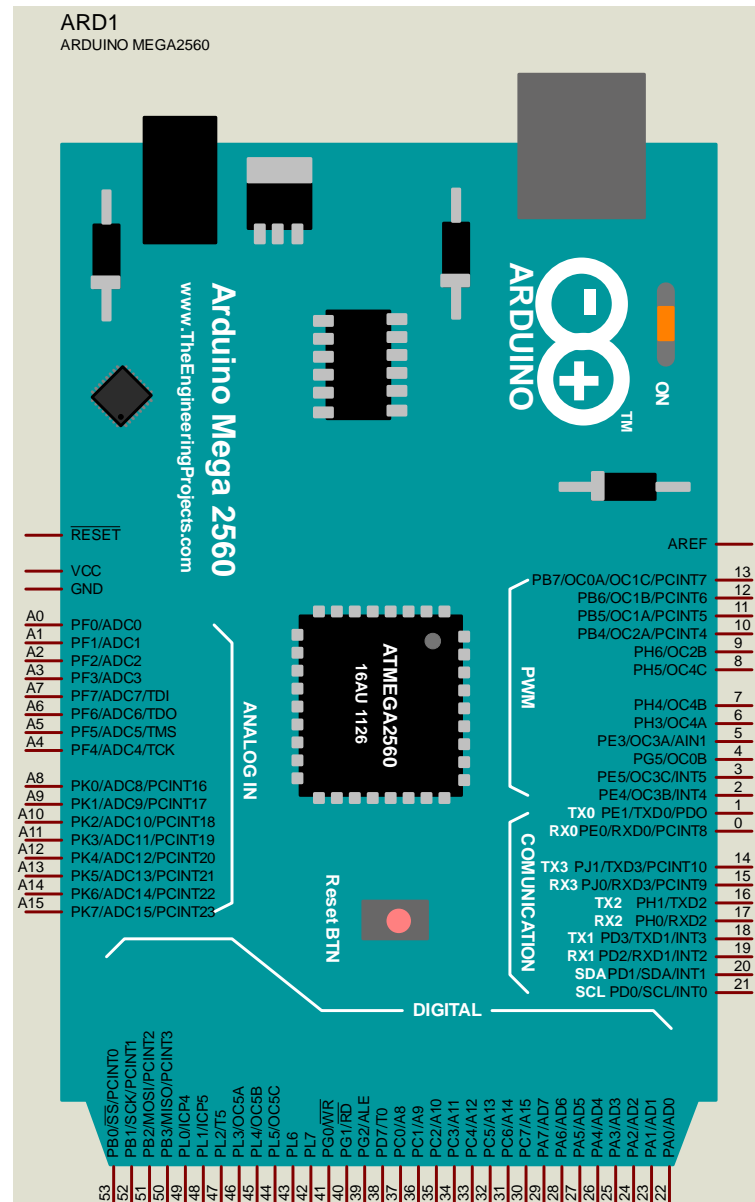


Figure 3-3: the Arduino mega

3.2.4 The Servo motor

A servomotor is used in the simulation as actuator. It consists of a motor, a position sensor and an electronic regulator, wired with the ground, Vcc and to the output of the Arduino.

The operation of the motor is controlled by the position of the axis. It is controlled by indicating which angle must take its axis (between 0 and 180°). The motor then starts until the end position is reached.

In the screenshot below we have showed the servomotor.

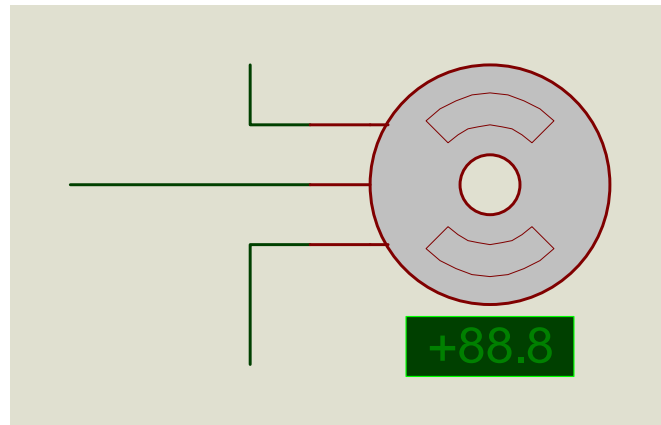


Figure 3-4: the servo motor

3.2.5 The whole Schematic diagram of the Simulated system

We will show the whole simulated system which will perform the comparison between the sum of LDR's one plus three and two plus four for the X axis, the microcontroller will compare the two values, motor will turn clockwise until the two values will be equal, later on, it will check the sum of LDR's three plus four and two plus one for the Y axis the motor will turn up down also until the two values will be equal. The figure 3-5 interfaces that system.

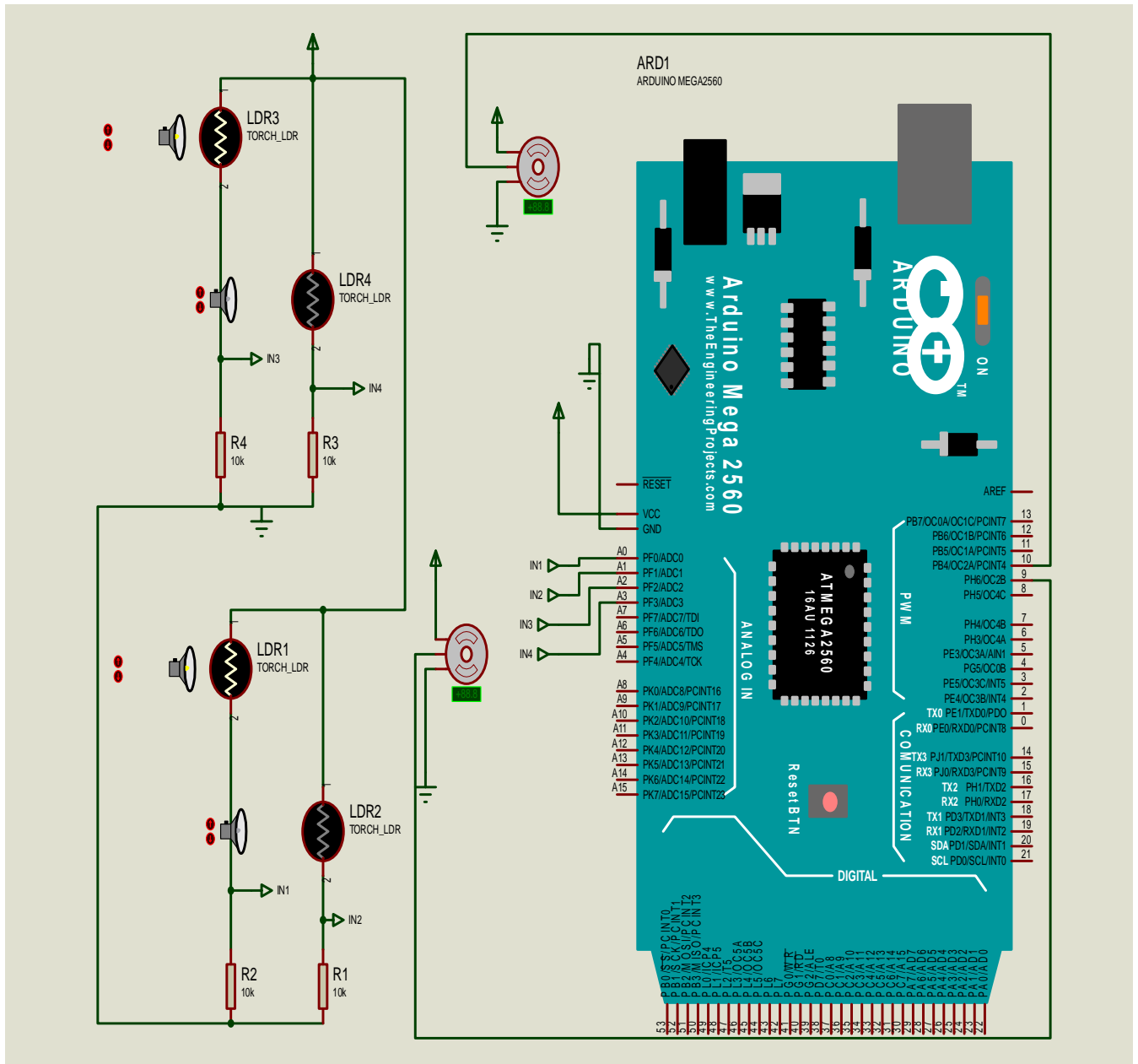


Figure 3-5: The whole circuit built by Proteus

3.3. The Flow code

The Arduino Mega 2560 is programmed by this Flowcode to perform the tracking system as follows

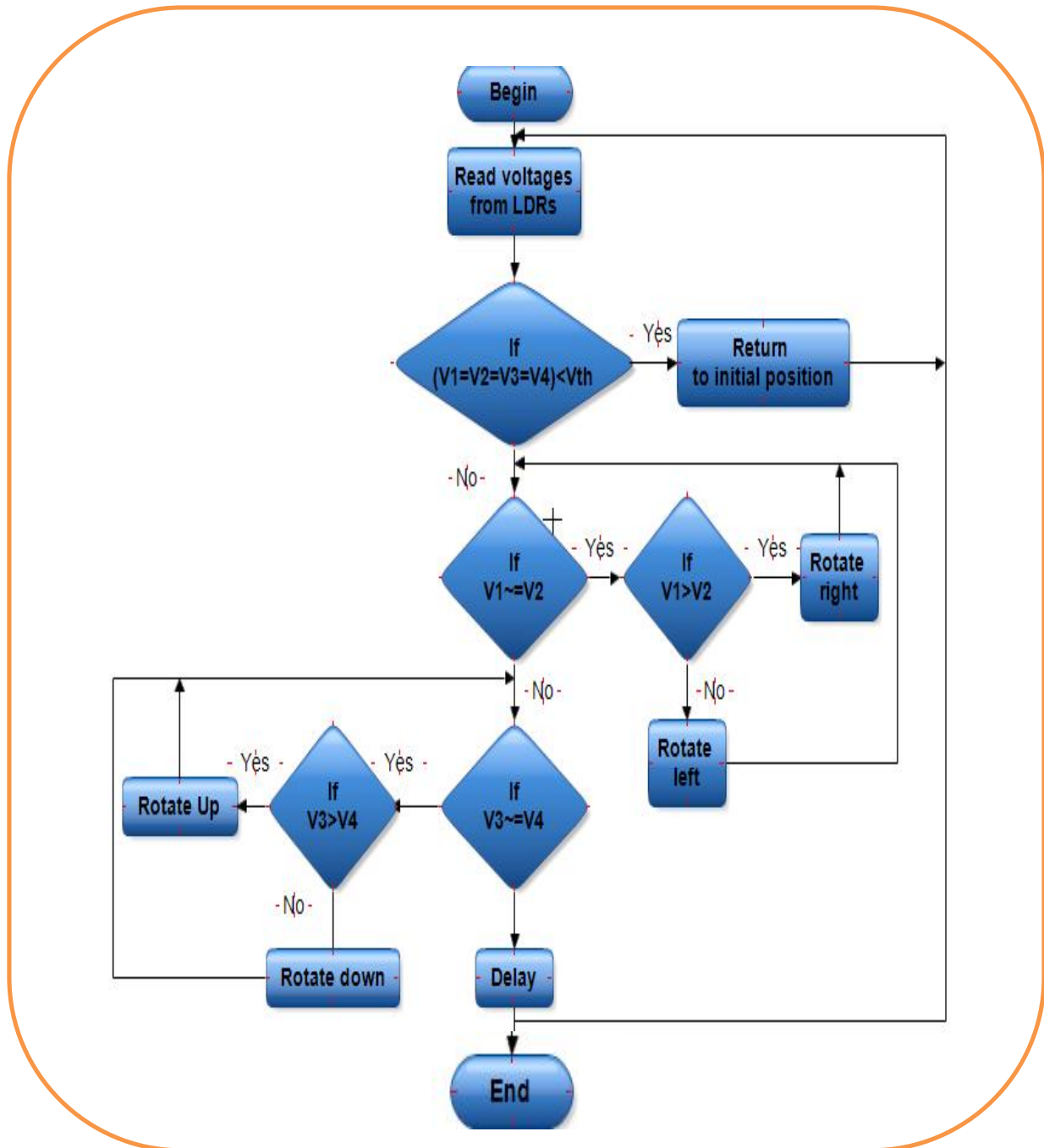


Figure 3-6: Flowchart of the simulated system.

3.4. The simulation results

The simulation results of the dual axis sun tracker were obtained in a form of displacement of the servomotor and we are mainly interested in keeping the position perpendicular to the light intensity throughout all the time simulating the cell solar position in order to make it more efficient and the comparison between the four cases (when the motor turns up, down, left and right) is illustrated by the next figure.

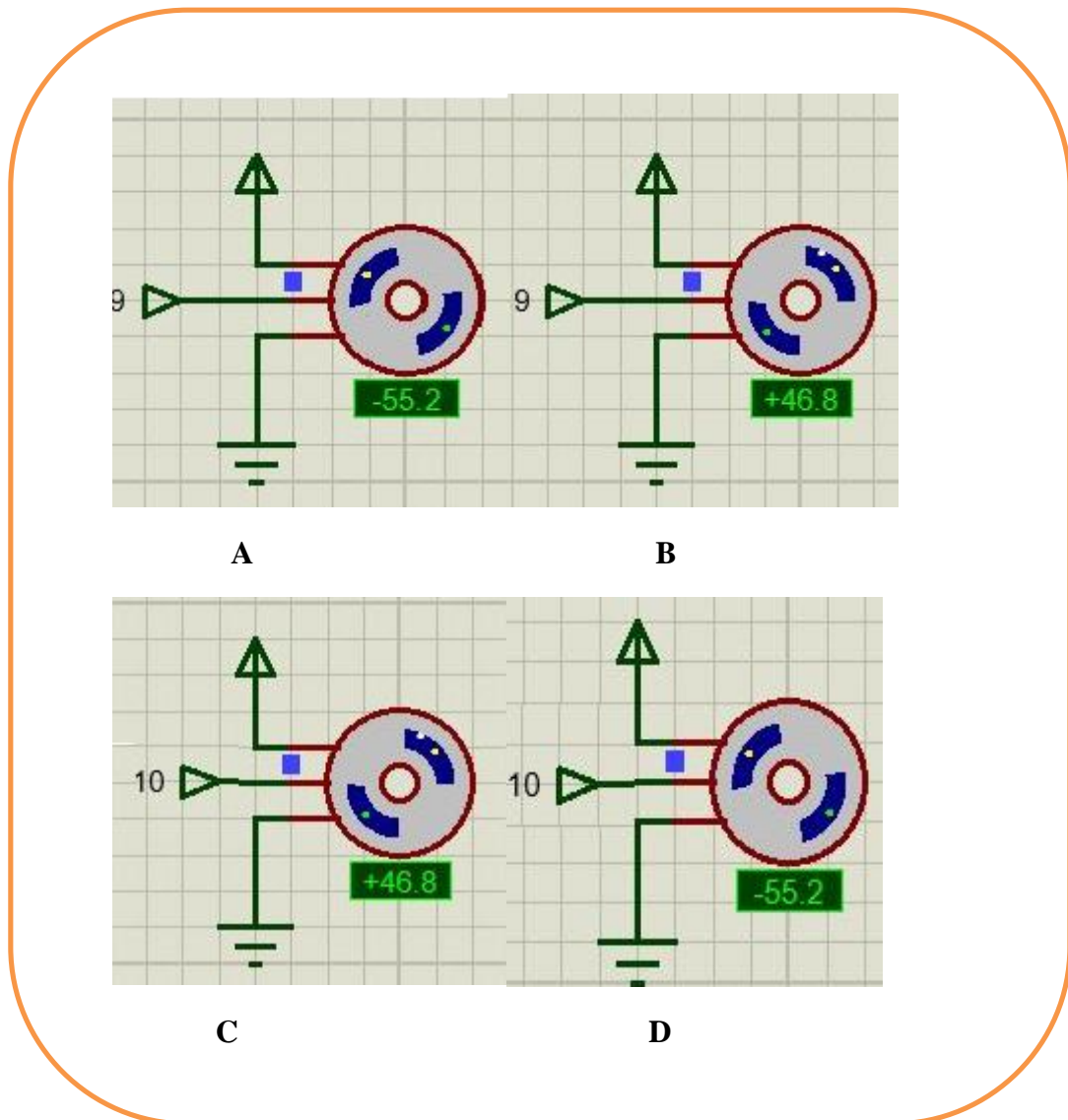


Figure 3-7: Result of simulated.

As we can see each snap represents one case of the rolling of the mechanism

- A : The motor turns to the left
- B : The motor turns to the right

- C : The motor turns up
- D : the motor turns down .

And finally we can say that we reached the desired simulation and it is realized physically, and that's we will illustrate in the next chapter.

chapter IV

Implementation of the system

4.1. Introduction

Most of the Dual Axis Trackers, are designed to rotate about a vertical axis to follow the sun from sunrise to sunset, in addition to a horizontal axis in order to change the tilt angle formed by the surface of the panel and the horizon, in our implementation we designed a tracker which follows the sun automatically in both sides the zenith and the azimuth that has a fast tracking capability under the change in the weather conditions (Partial shading). To evaluate the performances of the system we used two solar cells, one static and other implanted in the tracker system, then we measure the power absorbed from each one using a certain special sensors that will be mentioned later, finally, we analyze the data extracted from the outputs of both solar cells and store them on a SD card with a specific module.

4.2. The Tracker design and Choice of Components

In this section we are going to show some sections that will illustrate how the device is made as well as how it operates.

4.2.1 The sensor device

We assembled a sensor device by composing a separated four parallel of a light dependent resistor (LDR) associated in series with a 10k resistor as we did in the simulation part, the figure 4-1 shows the circuit of the voltage divider, where

$$V_{out} = \left(\frac{R}{R + R_{LDR}} \right) \cdot V_{in}$$

Where, **V_{in}** : sensor supply voltage (5v) , **R_{LDR}** : Resistance of the LDR.

V_{out} : Voltage of the sensor output and **R** : Resistance in (k Ω).

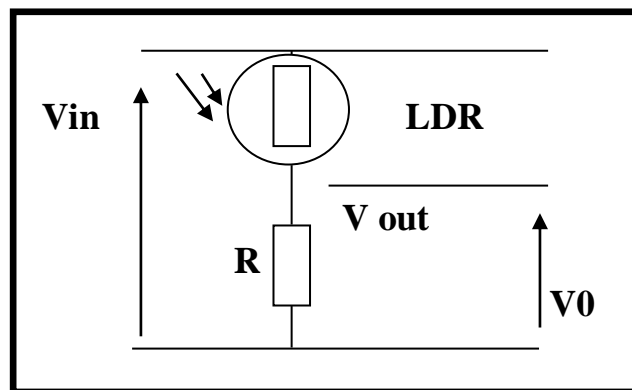


Figure 4-1:LDR resistor connection as voltage divider.

The most important device in this sensor is the LDR which is a dipole that decreases its resistance when illuminated. Placed in a closed circuit, it modifies the intensity of the current under the action of light. It operates as follows; A low-temperature semiconductor crystal contains few free electrons. The conductivity of the crystal is very low, close to that of an insulator. When the temperature of the crystal increases. More and more electrons that were immobile in the covalent bonds escape and can participate in the conduction.

At room temperature if the same semiconductor crystal is subjected to a light radiation, the energy provided by the photons may be sufficient to release some electrons used in the covalent bonds between atoms of the crystal. The higher the luminous flux will be, the more the number of free electrons to ensure the conduction will be large, so the resistance of the LDR is inversely proportional to the light received. The sensitivity depends on the frequency of the light radiation. To convert this variation of light into a voltage we used the voltage divider circuit and here in figure 4-2 we can see the LDR used.

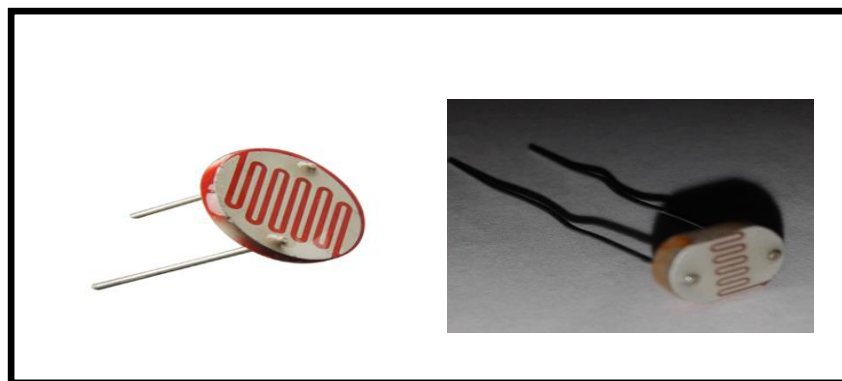


Figure 4-2:Photoresistor “Light Dependent Resistor”

Also the arrangement of the four LDR must be in such way which is clarified later to control the execution of the command correctly, For the four cases mentioned above, it is essential to consider three parameters when disposing the LDR sensors. The angle " ϵ " of the solar shadow which is in function of the height " H " of the wall, and the distance " d " which separates it from the sensor as shown in **Figure4-3**. Indeed " ϵ " is the trigger threshold angle or threshold of the solar shadow

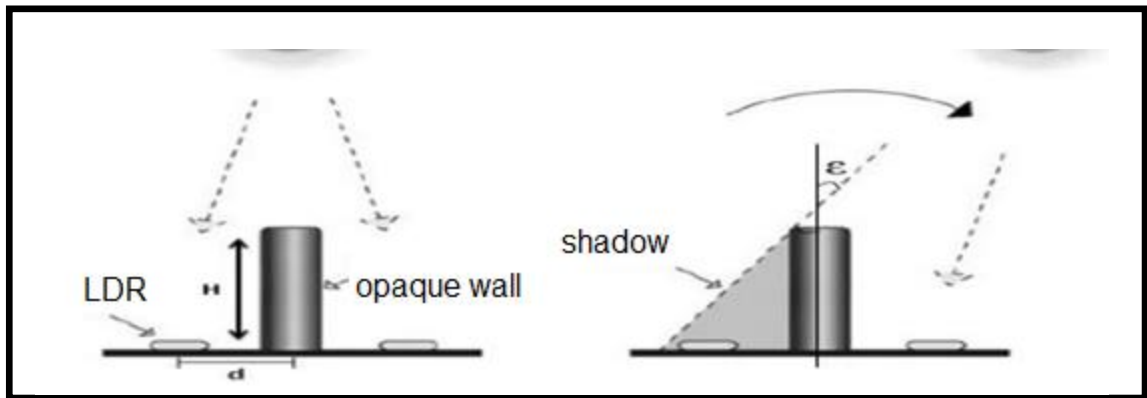


Figure 4-3: Arrangement of LDR sensors for a single-axis follower.

These parameters are defined by the following equations:

$$\text{➤ } \varepsilon = \text{Arc sin } \frac{d}{\sqrt{(d^2 + H^2)}}$$

$$\text{➤ } H = \frac{d}{\tan \varepsilon}$$

where

- H Height of the wall on (cm).
- D: distance between the wall and the LDR light sensor in (cm).
- ε: angle of the solar shadow in (°)

4.2.2 The servomotor

We choose servomotor **SG90** as it appears in figure 4-4. and involve it in the system to rotate the mechanism in the both sides; up, down and left, right.

This component is controlled by indicating which angle must take its axis (between 0 and 180 °). The motor then starts until the end position is reached.

A servomotor consists of three wires:

- Brown: GND
- Red: V cc (4.8 to 6v).
- Yellow: the signal command.



Figure 4-4: servomotor SG90.

The servomotor [21] contains:

- A DC motor.
- A reducer at the end of this engine to have torque
- A potentiometer (or an encoder) that induces a variable resistance according to the angular position of output, therefore the potentiometer and linked to the axis of the motor
- A servo circuit.

This motor must be connected to the Arduino as follow in figure 4-5.

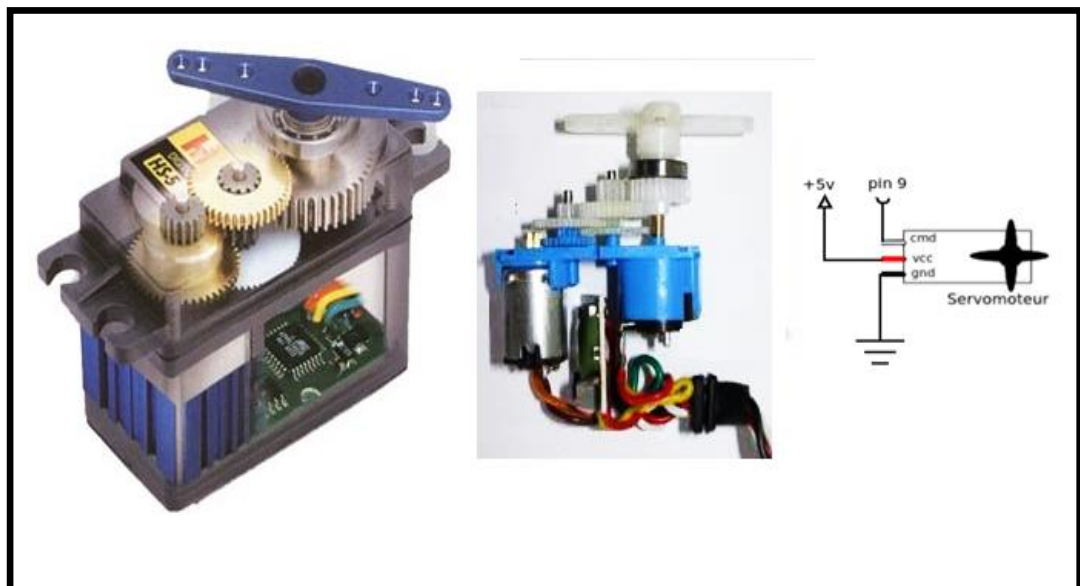


Figure 4-5: Servomotor pinout.

The control signal of a servomotor is a PWM signal of frequency 50Hz and whose high level must be between 1 and 2ms (in theory) as shown in figure 4-6

- 1ms: -90° angle of exit
- 1.5ms: 0° output angle
- 2ms: $+90^\circ$ in exit angle

PWM (Pulse Width Modulation) is used to control the signal of a servomotor. But, unlike DC motors, it is the duration of the positive pulse that controls the position, rather than the speed, of the servomotor shaft. The value of the neutral pulse depends on the servocontrol keeps the servo motor shaft in the middle position. The increase in the pulse value will go around the servomotor counterclockwise, and a shorter pulse will pass clockwise from the shaft.

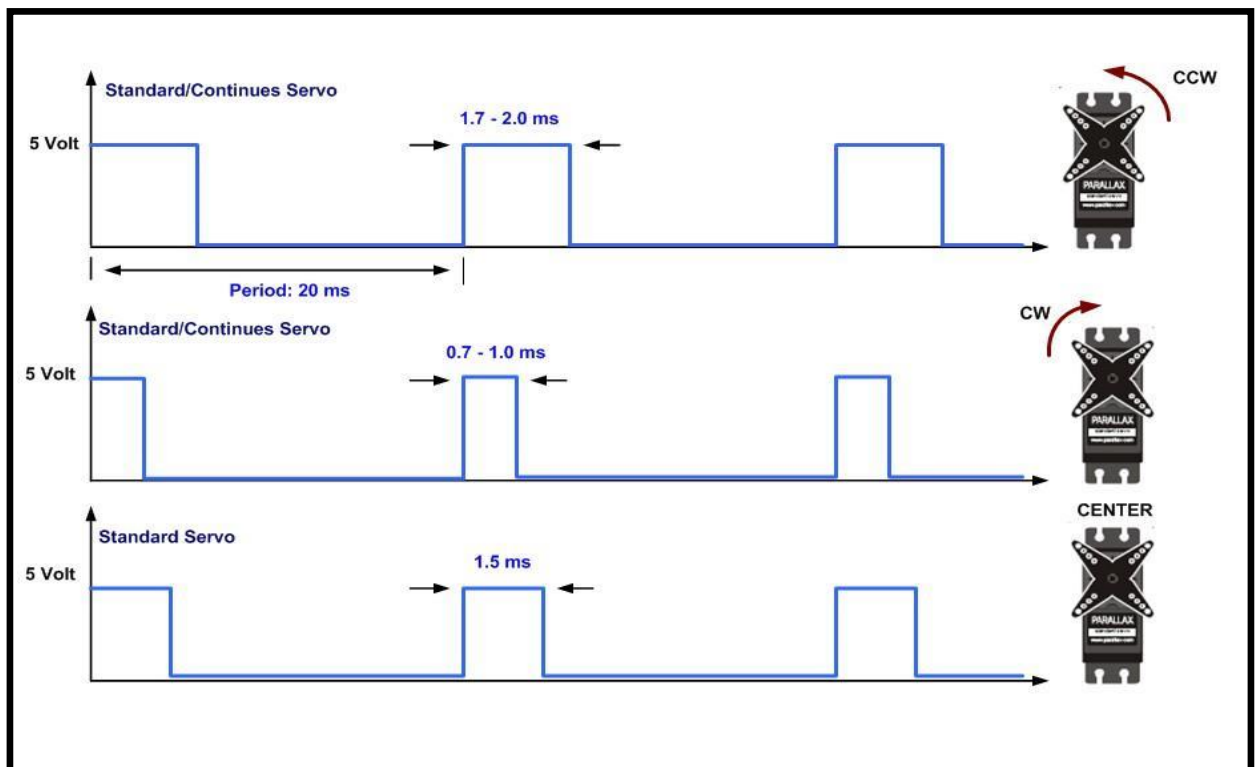


Figure 4-6: Angular displacement of a servomotor.

4.2.3 Arduino MEGA2560

This system is controlled by a microcontroller called "Arduino MEGA 2560", the advantage of this circuit is to minimize the surface of the electrical cards so we minimize the use of quantities of electronic components.

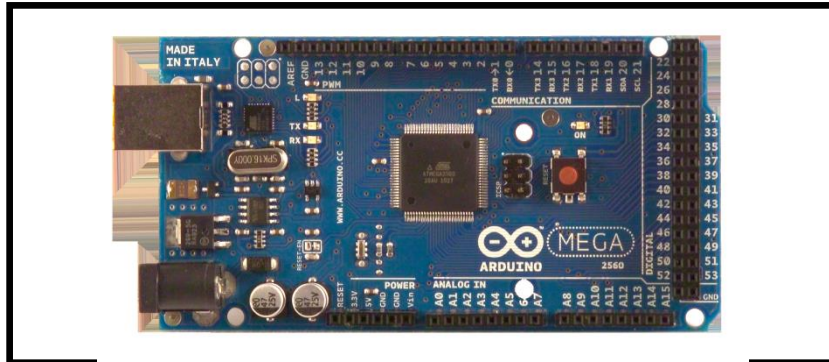


Figure 4-7: The card Arduino MEGA2560.

The Arduino Mega 2560 used in this work is a microcontroller board based on the ATmega2560. It has 54 digital input/output pins (of which 14 can be used as PWM outputs), 16 analog inputs, 4 UARTs (hardware serial ports), a 16 MHz crystal oscillator, a USB connection, a power jack, an ICSP header, and a reset button. It contains everything needed to support the microcontroller; simply connect it to a computer with a USB cable or power it with a AC-to-DC adapter or battery to get started. The Mega is compatible with most shields designed for the Arduino Duemilanove or Diecimila.

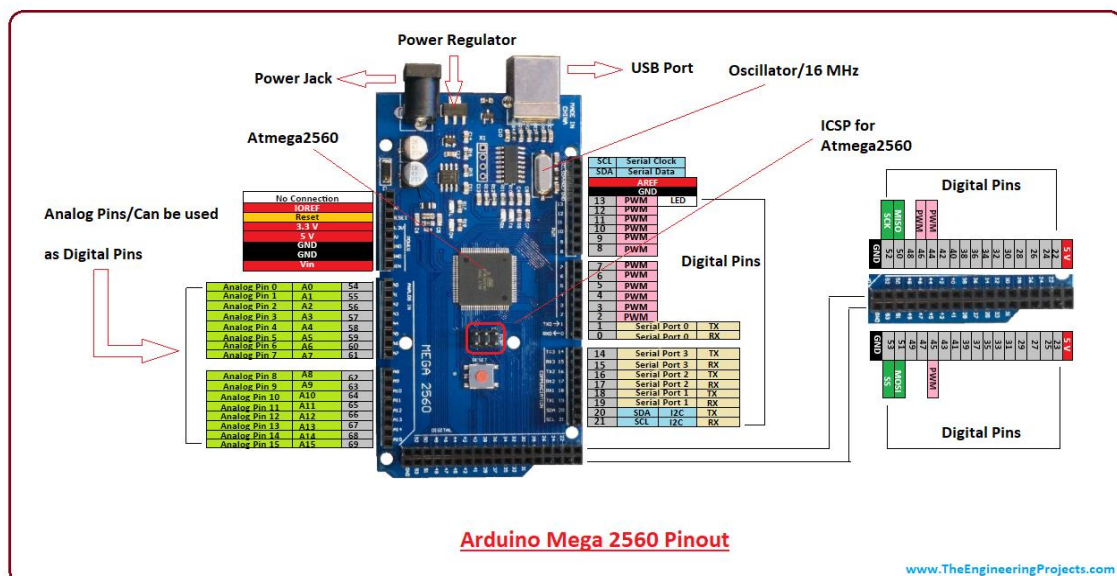


Figure 4-8: Arduino Mega Card Features.

The microcontroller ATmega2560 is a microcontroller of the AVR family whose programming can be done in C language[22].

The Features of Adriano Card used in our implementation are summarized in the following table:

Operating Voltage	5V
Input Voltage (recommended)	7-12V
Input Voltage (limits)	6-20V
Digital I/O	Pins 54 (of which 14 provide PWM output)
Analog Input Pins	16
DC Current per I/O Pin	40 mA
DC Current for 3.3V Pin	50 mA
Flash Memory	256 KB (8 KB used by bootloader SRAM)
EEPROM	4 KB
Clock Speed	16 MHz

Table 4.1: Arduino card features

4.2.4 The Data logger module (The SD Card module)

In this implementation we used the SD card module as a data acquisition tool, which is especially useful for projects that require data logging. The Arduino can create a file in an SD card to write and save data using the SD library.

There are different models from different suppliers, but they all work in a similar way, using the SPI communication protocol [23].



Figure 4-9: The SD card module

The following table summarized the way of interfacing the SD Card module to the Arduino Mega 2560.

SD card module	Wiring to Arduino Mega
VCC	3.3V or 5V (check module's datasheet)
CS	53
MOSI	51
CLK	52
MISO	50
GND	GND

Table4-2: Interfacing the SD Card module to the Arduino

4.2.5 The Current sensor module ACS712

To get the power of a solar cell, we need the values of the current of the resistor connected in parallel with the cell that can be measured using this module.

The **ACS712 Module** uses the famous **ACS712 IC** to measure current using the Hall Effect principle. The module gets its name from the IC (ACS712) used in the module, so for us final products use the IC directly instead of the module.

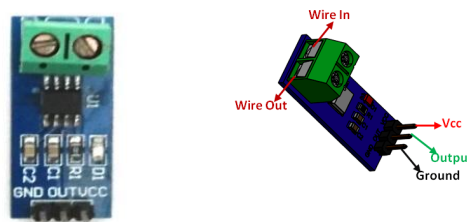


Figure 4-10: The Current sensor module ACS712

These ACS712 module can measure current AC or DC current ranging from +5A to -5A, +20A to -20A and +30A to -30A. we have to select the right range for our project since we have to trade off accuracy for higher range modules. This modules outputs Analog voltage (0-5V) based on the current flowing through the wire; hence it is very easy to interface this module with any microcontroller[24].

The Current sensor used can:

- Measure both AC and DC current
- Be available as 5A, 20A and 30A module
- Provide isolation from the load
- Easily integrate with MCU , since it outputs analog voltage

The scales Factor are 5A, 20A and 30A modules for 185mV/Amp, 100mV/Amp and 66mV per Amp respectively.

4.2.6 The voltage sensor module

The values of the voltage of the resistor connected in parallel with the solar cell are necessary to calculate the power, for this reason we used this module.

This module is based on resistance points pressure principle, and it can make the input voltage of red terminal reduce 5 times of original voltage. The max Arduino analog input voltage is 5 V, so the input voltage of this module should be not more than $5\text{ V} \times 5 = 25\text{ V}$ (if for 3.3 V system, the input voltage should be not more than $3.3\text{ V} \times 5 = 16.5\text{ V}$). Because the Arduino AVR chip have 10-bit AD. so this module simulation resolution is 0.00489 V ($5\text{V}/1023$), And the input voltage of this module should be more than $0.00489\text{ V} \times 5 = 0.02445\text{ V}$.



Figure 4-11:The Voltage sensor module

The voltage sensor has Special Parameters[25] which are:

- Voltage input range: DC0-25 V
- Voltage detection range: DC0.02445 V-25 V
- Voltage analog resolution: 0.00489 V
- DC input interface: red terminal positive with VCC, negative with GND

4.2.7 DS1307 RTC module

In order to synchronize the acquisition stored in the SD card with the time, we used the DS1307 RTC module.

It is a low-power, full binary-coded decimal (BCD) clock/calendar plus 56 bytes of NV SRAM. Address and data are transferred serially through an I²C, bidirectional bus. The clock/calendar provides seconds, minutes, hours, day, date, month, and year information. The end of the month date is automatically adjusted for months with fewer than 31 days, including corrections for leap year. The clock operates in either the 24-hour or 12-hour format with AM/PM indicator[26].

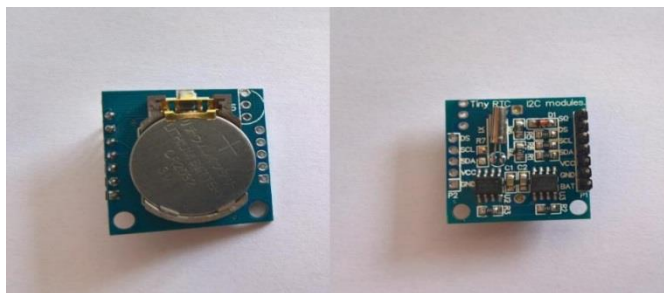


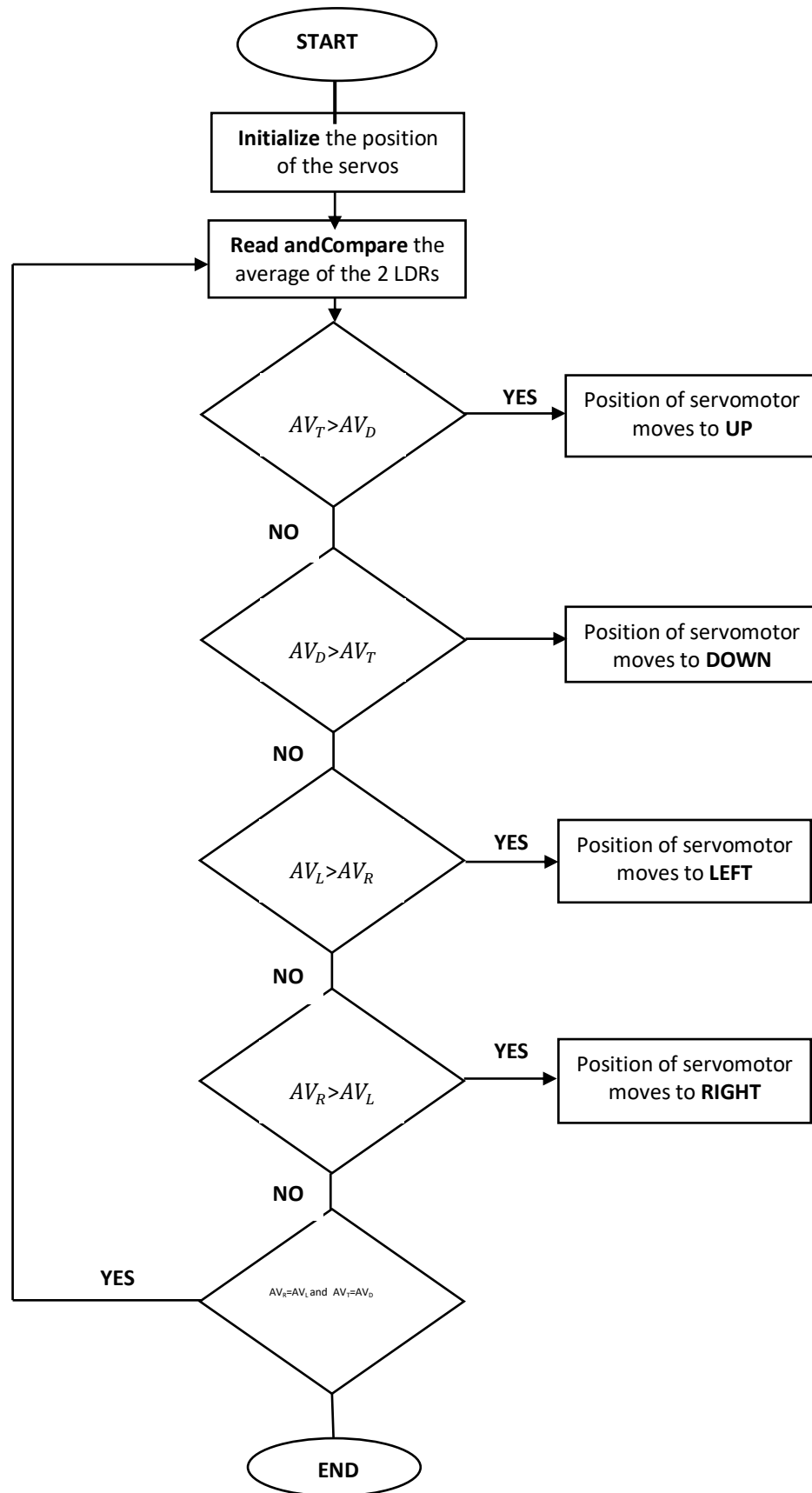
Figure 4-12:The DS13007 RTC Module

4.2.8 Solar cell

Solar cell, which is also called 'photovoltaic', is a device that converts light directly into electricity. There are many types of solar panel distinguished by their efficiency, price and temperature coefficient that are available in the market. Some of them are mono-crystalline, polycrystalline and thin film. The monocrystalline type of solar panel (figure 3-19) was selected for this project because it has the highest efficiency compared to other types. It is characterised by an Open Circuit Voltage of 6 V and a Short Circuit Current of 230 mA.



Figure 4-13:The solar cell



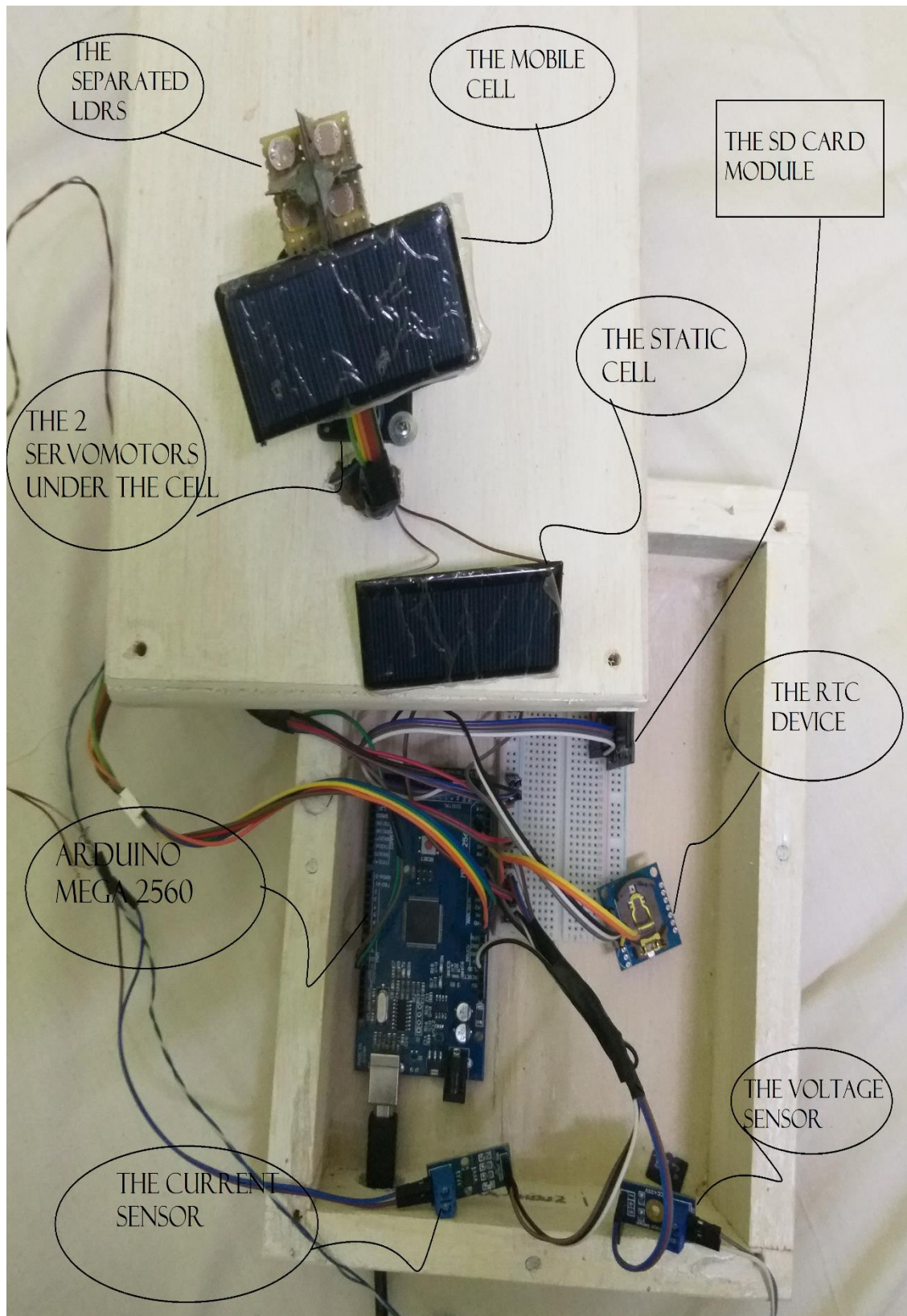


Figure4-15: The dual axis tracker

4.5. Experimental results and data analysis

4.5.1. Mobile versus static PV depending on light direction

The main component of our tracker is: Arduino MEGA, Light Dependent Resistors (LDRs); servo -motors; solar panel. The solar tracking system is done by Light Dependent Resistor (LDR). four LDR are connected to Arduino analog pin AO to A3 that acts as the input for the system. The analog value of LDR is converted into digital (Pulse Width Modulation) using the built-in Analog-to-Digital Converter.

The values of PWM pulse are applied to move the servos. The maximum light intensity captured by the one of the LDRs input will be selected and the servo motor will move the solar cell to the position of the LDR that was set-up in the programming. There are three points of motor rotation; 0; 90 and 180 degrees. The positions of LDR are divided into four positions; which are; right; left; up and down. The 4 positions allow the highest intensity of sunlight to be can be detected. The microcontroller gets an analog input from the Light Dependent Resistor (LDR) which is then converted into digital signal by Analog-to-Digital converter. The movement of the solar cell is determined by the output given to the servo motor.

The twosensors allow us to get the power of the both cells; the static and which is equipped with the tracker and store that data in a SD card.

The proposed model was constructed successfully and tested, as we can see in figure 4.16a when the light is perpendicular to both cells, we obtain almost the same output as well as the same position.

Contrariwise, when the light is not direct exposed, the tracker moves in such way to be perpendicular to the lightas wedepict in figure 4-16b,14-16c and 4,16d respectively when the light is situated left, right and up to the two cells.

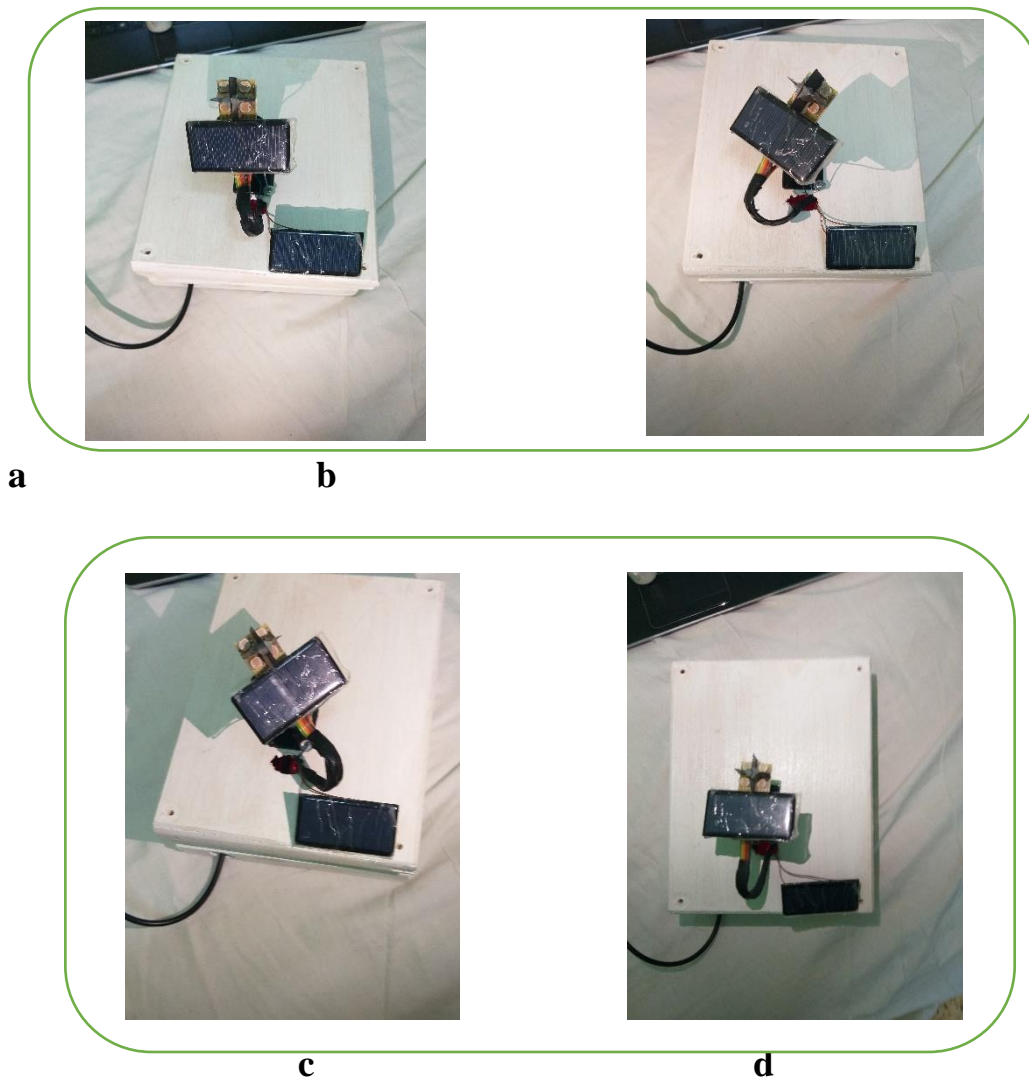


Figure4-16: The tracker after operating

4.5.2. Data analysis

To evaluate the performances of the two PV systems, we have extracted the values of the electrical current and voltage acquiring with a 30 minutes sample rate using the current sensor on the fixed cell, and the voltage sensor on the tracker, with a 10 k resistor in each cell connected on series with this last.

We fixed the first solar cell directed to the south with an angle equal to 36 degrees (static cell) and we placed the second on the tracker (tracking cell)

The measurements were performed in the day interval 11.00–14.00, we have obtained the following tables 4-3 & 4-4 which show the current, voltage and power values received from both the static and tracking cells.

Time	11:00	11:30	12:00	12:30	13:00	13:30	14:00
Current(mA)	0.471	0.479	0.482	0.485	0.491	0.491	0.480
Voltage(V)	4.71	4.79	4.82	4.85	4.91	4.91	4.80
Power(mW)	2.22	2.30	2.32	2.35	2.41	2.41	2.31

Table 4-3: Variation of power output of the static (fixed) cell VS time

Time	11:00	11:30	12:00	12:30	13:00	13:30	14:00
Current(mA)	0.575	0.574	0.578	0.581	0.579	0.582	0.584
Voltage(V)	5.75	5.74	5.78	5.81	5.79	5.82	5.84
Power(mW)	3.31	3.29	3.34	3.38	3.35	3.39	3.41

Table 4-4: Variation of power output of the cell on the tracker VS time

We plotted the power VS time curve for the two systems, we have got the following curve:

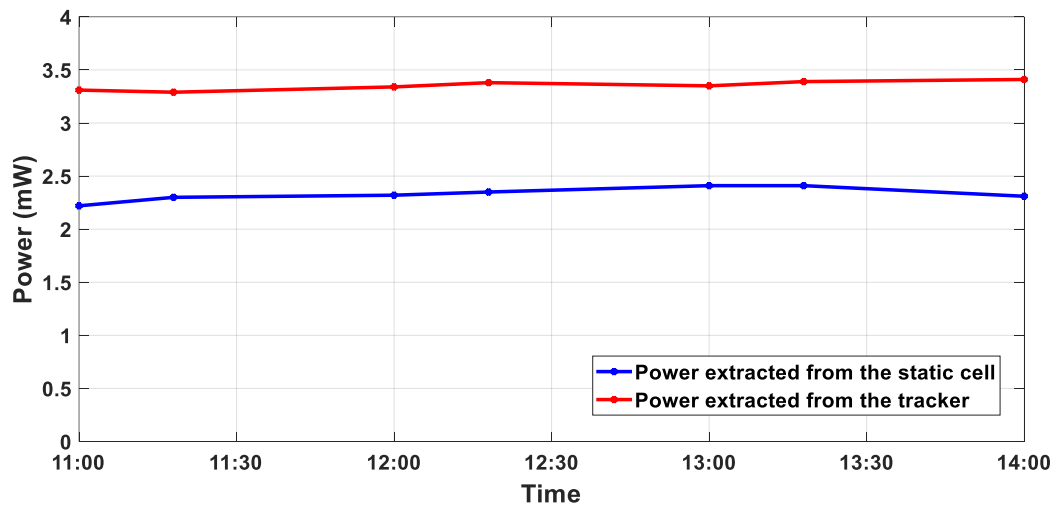


Fig 4-17: The comparison of power curves for both the static and tracking panel.

The total power of static panel throughout this recorded period is 16.32mW. Meanwhile the total power of tracking panel throughout this period is 23.47mW. Therefore, the average power gain by tracking panel over fixed panel = 43.81%

The efficiency of dual-axis tracker system is higher when compared with single-axis tracker system.

Discussion

Although a tracker might be highly efficient and provide a good average energy gain compared to an immobile system or a single axis system, this is not enough yet to claim the system is beneficial over its alternatives. The added tracking component to the system must provide enough power gain that there is either an immediate payback or the payback period is less than the lifetime of the system.

In Addition, it was mentioned in numerous papers [27] that the use of trackers is beneficial only if we use them for a large system composed of several solar panels, for this reason, the economic study is not carried on our small prototype, instead, we will discuss the economic aspects for real system.

According to researches conducted in Bouzereah and Ghardaia [28], The dual Axis Tracker have a 30% gain over the system oriented to the south and with a tilt angle equal to the latitude angle of those places, which means that 3 solar panels placed on a dual axis will produce same energy as 4 fixed panels and given that those panels are quite expensive and relatively light to place more units on a same tracker, the use of tracker is a good option.

We can control many trackers using only one microcontroller which reduce the overall cost. a good design of structure supporting the panels will reduce the amount of required torque, therefore, we can buy smaller and cheaper actuators.

Conclusion



CONCLUSION

As a means to provide an efficient solar distributed generation system; this master thesis presented a scaled down active dual-axis solar tacker system design. The system was constructed and operated successfully. The built prototype ensures design feasibility. It was farther tested in Proteus. The results show an average power gain of 43.81% compared to an immobile solar panel. The advantages of the proposed dual axis tacker are

- (i) it uses servomotors; a high performance alterative as the driving device for the solar panel and consumes less power as compared to stepper motor Ipennanent magnet d.c motors with gears.
- (ii) The proposed tracker is cost effective; simple and efficient; operates automatically.
- (iii) The controlling unit used is an inexpensive Arduino Mega; a single-board microcontroller; an open source electronics platform based on easy-to-use hardware and software.
- (iv) The method used for data acquisition and the storage way can help to analyze the output of the panel as well as check and control the state of the panel.

The developed solar tacker can be used for small scale solar PV power generation at remote places. It can also be used in solar street lighting system or any other stand-alone solar PV application. The running efficiency of the solar PV panel can be farther enhanced by developing an automatic dust sensor wiper for maintaining absorption of solar radiations by the solar PV panel.

Abbreviations:

PV: Photovoltaic

DC: Direct Current.

AC: Alternative Current.

MPPT: Maximum Power Point Tracking.

HSAT: Horizontal Single Axis Tracker.

VSAT: Vertical Single Axis Tracker.

TSAT: Tilted Single Axis Tracker.

PASAT: Polar Aligned Single Axis Tracker.

TTDAT: Tip-Tilt Dual Axis Tracker.

AADAT: Azimuth Altitude Dual Axis Tracker.

N-S: North - South.

E-W: East – West.

NREL: National Renewable Energy Laboratory.

GPS: Global Positioning System.

LDR: Light Dependent Resistor.

PCB: Printed Circuit Board.

V_{cc} : Voltage at the Common Collector.

V_{out} : The Output Voltage.

V_{in} : The Input Voltage.

R : Resistor.

R_{LDR} : The LDR resistor.

GND: The **G**round.

PWM: **P**ulse **W**idth **M**odulation.

AVR: **A**dvanced **V**irtual **RISC**.

RISC: **R**educed **I**nstruction **S**et **C**omputing.

SPI: **S**erial **P**eripheral **I**nterface.

BCD: **B**inary **C**oded **D**ecimal.

A.1 The MPPT Algorithms:

A.1.1 Fractional open-circuit voltage:

This method uses an approximate linear relationship between the MPP voltage (V_{MPP}) and the open circuit voltage (V_{OC}), which is function of the irradiance and the temperature:

$$V_{MPP} \approx K_1 V_{OC}$$

Where K_1 is a constant depending on the characteristics of the PV panel and it has to be determined by conducting several experiments and determine the V_{MPP} and V_{OC} for different levels of irradiation and different temperatures. The constant K_1 has been reported to be between [0.71; 0.78].

Once the value of the constant K_1 is known, the MPP voltage (V_{MPP}) can be determined periodically by measuring V_{OC} . In doing so the power converter has to be shutdown momentarily which causes a loss of power. In addition, this method is not capable of reaching the real MPP point because the relationship is only an approximation.

Depending on the application, this technique can be used because it's very easy to implement and it is cheap (it does not require DSP or microcontroller control and just one voltage sensor is used), however, this method is not valid under partial shading because the value of K_1 changes.

The Fig-A.1- shows the scheme of the Fractional open-circuit voltage method:

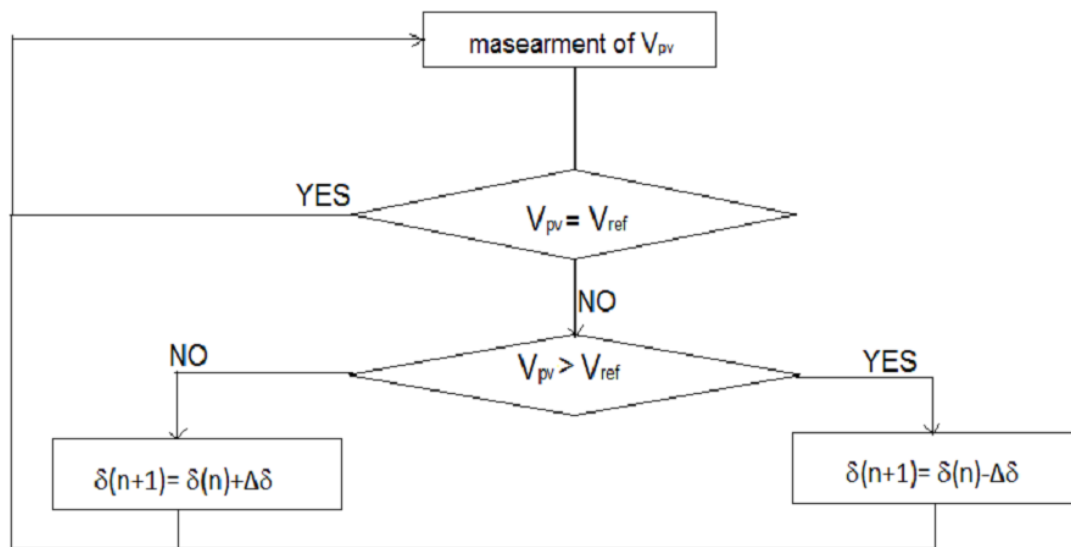


Fig-A.1-: Flowchart of the Fractional open-circuit voltage algorithm.

A.1.2 Fractional short-circuit current:

In the same manner of fractional open-circuit voltage, there's a relationship, under varying atmospheric conditions, between the short circuit current I_{SC} and the MPP current, I_{MPP} as shown by:

$$I_{MPP} = K_2 * I_{SC}.$$

Where, the constant K_2 has been reported to be between [0.78; 0.92].

Measuring the short circuit I_{SC} current while the system is operating presents a problem. It is usually requires adding an additional switch to the power converter to periodically short the PV array and measure I_{SC} . One other handicap is that the real MPP is not reached because the proportional relationship is an approximation. Fig-A.2- shows the scheme of the Fractional short-circuit current algorithm.

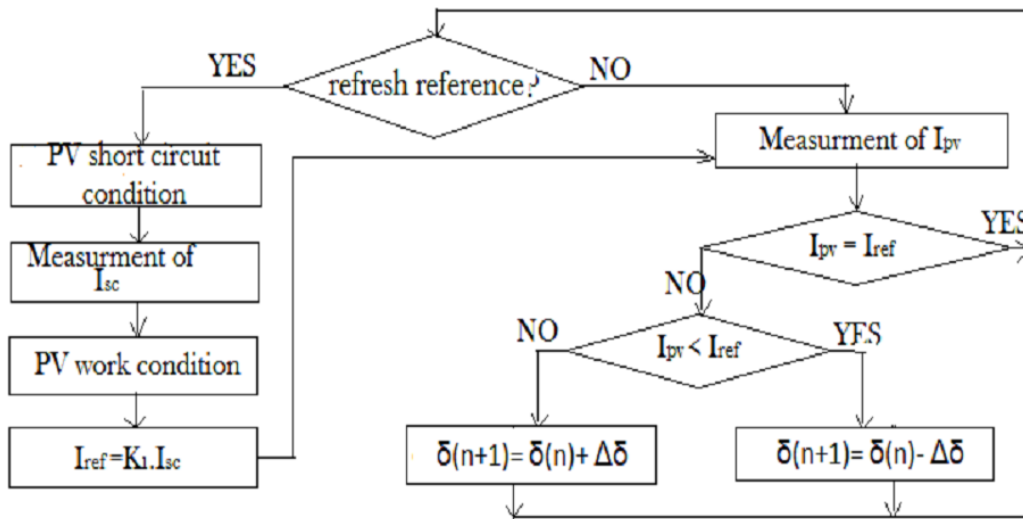


Fig-A.2-: Flowchart of the Fractional short-circuit current algorithm.

A.1.3 Hill-climbing techniques:

The Perturb and observe (P&O) technique and incremental conductance (InCond) are both based on Hill-climbing principal, which consists of moving the operating point in the direction in which the power increases. Hill-climbing techniques are the most popular MPPT methods due their ease of implementation and the good performance when the irradiance is constant. The advantages of both methods are the simplicity and the low computational power needed.

A.1.3.1 Perturb and observe (P&O):

The P&O technique involves a perturbation in the duty cycle of the power converter (DC/DC converter), the sign of the last perturbation and the sign of the last increment in the power decide what the next perturbation should be. Such that if there is an increment in the power, the perturbation should be kept in the same direction and if the power decreases, then the next perturbation should be in the opposite direction.

Based on these facts, the algorithm is implemented; the process is repeated until the MPP is reached. Then the operating point oscillates around the MPP and this problem is also common to the InCond method, a scheme of the algorithm is shown in the Fig-A.3-:

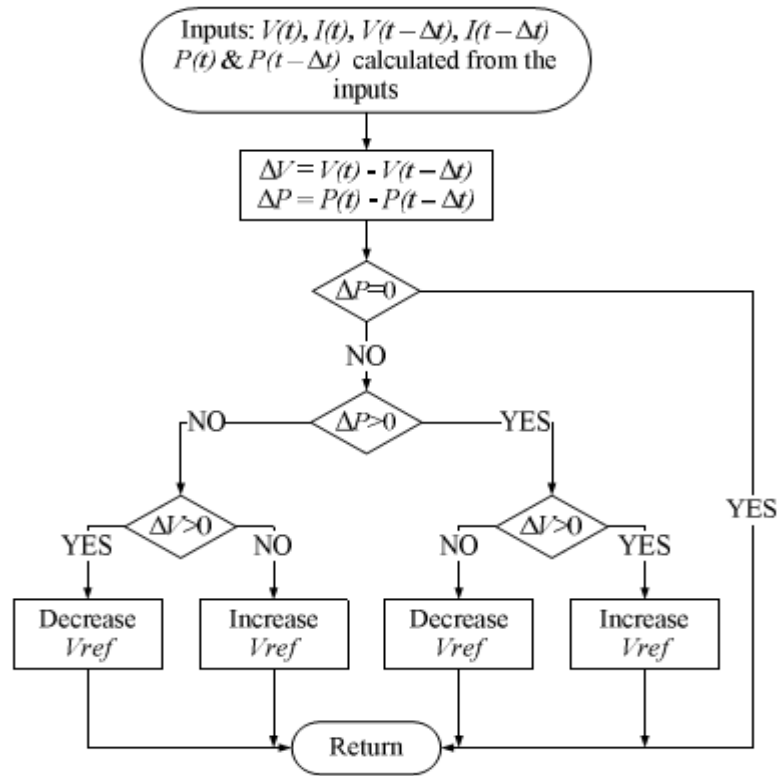


Fig-A.3-: Flowchart of the P&O algorithm.

A.1.3.2 Incremental conductance method:

Appendix A

The Incremental conductance (InCond) method is based on the fact that the sum of the instantaneous conductance I/V and the incremental conductance $\Delta I/\Delta V$ is zero at the MPP, negative on the right side of the MPP, and positive on the left side of the MPP. This can be summarized as follows:

$$\left\{ \begin{array}{l} I/V + \Delta I/\Delta V < 0, \text{ right of MPP.} \\ I/V + \Delta I/\Delta V = 0, \text{ at MPP.} \\ I/V + \Delta I/\Delta V > 0, \text{ left of MPP.} \end{array} \right.$$

From these characteristics, it's seen that $|dP/dV|$ decreases as MPP is approached and increases when the operating point moves away from MPP. This relation can be given by:

$$\left\{ \begin{array}{l} dP/dV < 0, \text{ right of MPP.} \\ dP/dV = 0, \text{ at MPP.} \\ dP/dV > 0, \text{ left of MPP.} \end{array} \right.$$

In order to obtain the operating MPP, dP/dV should be calculated:

$$\frac{dP}{dV} = \frac{d(V I)}{dV} = I + V \frac{dI}{dV}$$

This method suffers from the same drawbacks of the P&O method, especially that it can easily lose to track the MPP when there's a rapidly change in the irradiance, so the changes in the voltage and current are not only due to the perturbation of the voltage. As a consequence it is not possible for the algorithms to determine whether the change in the power is due to its own voltage increment or due to the change in the irradiation.

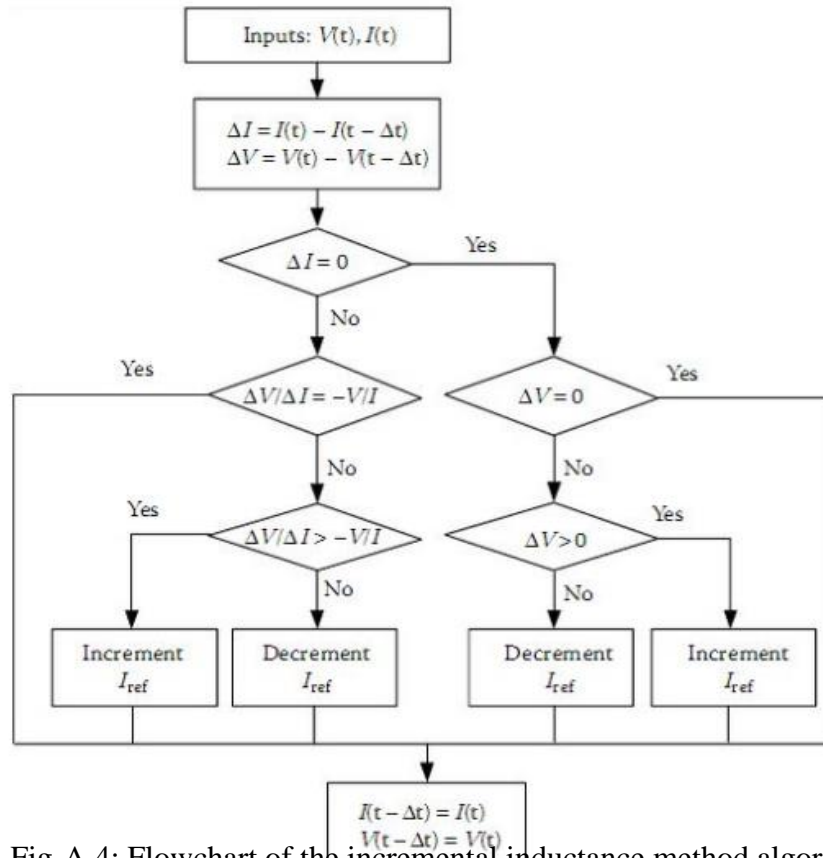


Fig-A.4: Flowchart of the incremental inductance method algorithm.

A.1.4 Neural networks:

Neural networks can be used in the MPPT Algorithm, and it's well adapted to microcontrollers and DSP. The simplest example of the NN has three layers the input layer; the hidden layer and the output layer; as shown in the Fig-A.5-. More complicated NN are built by adding more hidden layers. The input variables can be variables of the PV array such as V_{OC} and I_{SC} , the atmospheric data as irradiance and temperature or combination of these. The output is usually one or more reference signals like the duty cycle or the optimal voltage.

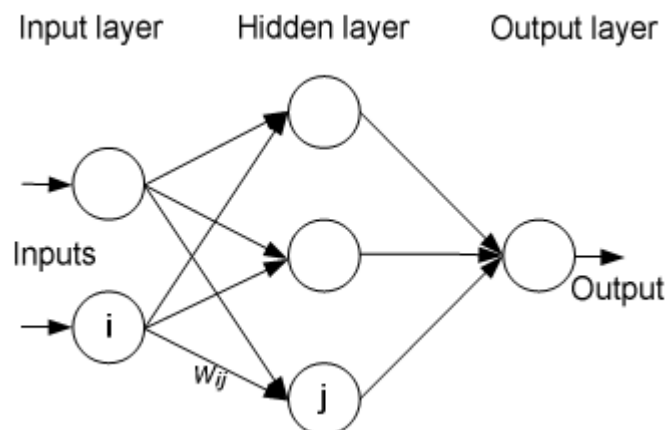


Fig-A.5-: The simplest artificial neural network.

Appendix A

The performance of the ANN depends on the functions used by the hidden layers and how well the ANN has been trained. The links between the nodes are all weighted. In fig-3.5- the weight between the nodes I and J are labeled as W_{ij} . The weights are adjusted in the training process. To execute this training, some data patterns between outputs and the outputs should be recorded over period of time, so that the MPP can be tracked accurately.

A.2.2 Arduino Code to operate the Tracking Mechanism:

```
#include <Servo.h> // include Servo library

// 180 horizontal MAX

Servo horizontal; // horizontal servo

int servoh = 180; // 90; // stand horizontal servo

int servohLimitHigh = 180;
int servohLimitLow = 65;

// 65 degrees MAX

Servo vertical; // vertical servo

int servov = 45; // 90; // stand vertical servo

int servovLimitHigh = 80;
int servovLimitLow = 15;

// LDR pin connections
// name = analogpin;

int ldrlt = 0; //LDR top left - BOTTOM LEFT <--- BDG
int ldrrt = 1; //LDR top right - BOTTOM RIGHT
int ldrlt = 2; //LDR down left - TOP LEFT
int ldrrd = 3; //ldr down right - TOP RIGHT
```

```
void setup()
{
  Serial.begin(9600);
  // servo connections
  // name.attach(pin);
  horizontal.attach(9);
  vertical.attach(10);
  horizontal.write(180);
  vertical.write(45);
  delay(3000);
}

void loop()
{
  int lt = analogRead(ldrLt); // top left
  int rt = analogRead(ldrRt); // top right
  int ld = analogRead(ldrLd); // down left
  int rd = analogRead(ldrRd); // down right

  // int dtime = analogRead(4)/20; // read potentiometers
  // int tol = analogRead(5)/4;

  int dtime = 10;
  int tol = 50;

  int avt = (lt + rt) / 2; // average value top
```

```
int avd = (ld + rd) / 2; // average value down

int avl = (lt + ld) / 2; // average value left

int avr = (rt + rd) / 2; // average value right


int dvert = avt - avd; // check the difference of up and down

int dhoriz = avl - avr; // check the difference of left and right


Serial.print(avt);

Serial.print(" ");

Serial.print(avd);

Serial.print(" ");

Serial.print(avl);

Serial.print(" ");

Serial.print(avr);

Serial.print(" ");

Serial.print(dtime);

Serial.print(" ");

Serial.print(tol);

Serial.println(" ");


if (-1*tol > dvert || dvert > tol) // check if the difference is in the tolerance else
change vertical angle

{

if (avt > avd)

{
```



```
servov = ++servov;

if (servov > servovLimitHigh)

{

    servov = servovLimitHigh;

}

}

else if (avt < avd)

{

    servov = --servov;

    if (servov < servovLimitLow)

    {

        servov = servovLimitLow;

    }

}

vertical.write(servov);

}


if (-1*tol > dhoriz || dhoriz > tol) // check if the difference is in the tolerance else
change horizontal angle

{

    if (avl > avr)

    {

        servoh = --servoh;

        if (servoh < servohLimitLow)

        {

            servoh = servohLimitLow;

        }

    }

}
```

```
}  
  
else if (avl < avr)  
{  
    servoh = ++servoh;  
    if (servoh > servohLimitHigh)  
    {  
        servoh = servohLimitHigh;  
    }  
}  
  
else if (avl = avr)  
{  
    // nothing  
}  
  
horizontal.write(servoh);  
  
}  
  
delay(dtime);  
  
}
```

References

References

- [1] Boyle, Godfrey. "Renewable energy." *Renewable Energy*, by Edited by Godfrey Boyle, pp. 456. Oxford University Press, May 2017.
- [2] Wüstenhagen, Rolf, and Michael Bilharz. "Green energy market development in Germany: effective public policy and emerging customer demand." *Energy policy* 34.13 (2006): 1681-1696.
- [3] Loeb, Norman G., et al. "Clouds and the earth's radiant energy system (CERES) energy balanced and filled (EBAF) top-of-atmosphere (TOA) edition-4.0 data product." *Journal of Climate* 31.2 (2018) : 895-918.
- [4] Kannan, Nadarajah, and Divagar Vakeesan. "Solar energy for future world:-A review." *Renewable and Sustainable Energy Reviews* 62 (2016): 1092-1105.
- [5] Jäger-Waldau, Arnulf. "Snapshot of photovoltaics— February 2018." *EPJ Photovoltaics* 9 (2018): 6.
- [6] Hoffmann, Winfried. "PV solar electricity industry: Market growth and perspective." *Solar energy materials and solar cells* 90.18-19 (2006): 3285-3311.
- [7] Liu, Wei, and Hong Li. "Improving energy consumption structure: A comprehensive assessment of fossil energy subsidies reform in China." *Energy policy* 39.7 (2011): 4134-4143.
- [8] Mousazadeh, H., Keyhani, A., Javadi, A., Mobli, H., Abrinia, K., Sharifi, A.. "A review of principle and sun-tracking methods for maximizing solar systems output". *Renewable and Sustainable Energy Reviews*. January 2009. Pages 1800, 1800, 1804, 1806, & 1812.
- [9] Luque. A and Hegedus. S. (2003).” *Handbook of Photovoltaic Science and Engineering*”. John Wiley & Sons Ltd, The Atrium, Southern Gate, Chichester, West Sussex PO19 8SQ, England, pp. 296-297.
- [10] TAMER T.N. KHATIB, A. MOHAMED and N. AMIN, ‘An Efficient Maximum Power Point Tracking Controller for Photovoltaic Systems Using New Boost Converter Design and Improved Control Algorithm’ *Issue 2, Volume 5, April 2010*.
- [11] M. Salhi, R. El-Bachtiri, ‘Maximum Power Point Tracking Controller for PV Systems using a PI Regulator with Boost DC/DC Converter’, *ICGST-ACSE Journal*, ISSN 1687-4811, Volume 8, Issue III, January 2009.
- [12] Chang, Tian Pau. "Output energy of a photovoltaic module mounted on a single-axis tracking system." *Applied energy* 86.10 (2009): 2071-2078.
- [13] Abdallah, Salah, and Salem Nijmeh. "Two axes sun tracking system with PLC control." *Energy conversion and management* 45.11-12 (2004): 1931-1939.

References

- [14] Sefa, I., Demirtas, M., Çolak, I.. "Application of One-Axes sun Tracking System". Energy Conversion and Management. 2009. Page 2710.
- [15] Roth, P., A. Georgiev, and H. Boudinov. "Cheap two axis sun following device." Energy Conversion and Management 46.7-8 (2005): 1179-1192.
- [16] Mehleri, E., Zervas, P., Sarimveis, H., Palyvos, J., Markatos, N.. "Determination of the optimal tilt angle and orientation for solar photovoltaic arrays". Renewable Energy. April 2010. Page 2469.
- [17] Wang, Jing-Min, and Chia-Liang Lu. "Design and implementation of a sun tracker with a dual-axis single motor for an optical sensor-based photovoltaic system." Sensors 13.3 (2013): 3157-3168.
- [18] Abdallah, Salah, and Salem Nijmeh. "Two axes sun tracking system with PLC control." Energy conversion and management 45.11-12 (2004): 1931-1939.
- [19] Mehleri, E., Zervas, P., Sarimveis, H., Palyvos, J., Markatos, N.. "Determination of the optimal tilt angle and orientation for solar photovoltaic arrays". Renewable Energy. April 2010. Page 2469.
- [20] M.Koussa, A.Malek, M.Haddadi , "Apport énergétique de la poursuite solaire sur deux axis par rapport aux système fixes. Revue des Energies Renouvelables Vol.10.
- [21] <https://components101.com/servo-motor-basics-pinout-datasheet> , visited on (2019-05-29 at 10:00 AM).
- [22] <https://www.robotshop.com/media/files/pdf/arduinomega2560datasheet.pdf> , visited on (2019-05-29 at 10:10 AM).
- [23] <https://store.fut-electronics.com/products/micro-sd-card-module> , visited on (2019-05-29 at 10:15 AM).
- [24] [https://www.elecrow.com/wiki/index.php?title=ACS712 Current Sensor- 5A](https://www.elecrow.com/wiki/index.php?title=ACS712_Current_Sensor-5A), visited on (2019-05-29 at 10:20 AM).
- [25] <https://www.instructables.com/id/Arduino-Voltage-Sensor-0-25V/> , visited on (2019-05-29 at 10:25 AM).
- [26] <https://datasheets.maximintegrated.com/en/ds/DS1307.pdf> , visited on (2019-05-29 at 10:30 AM).
- [27] Sefa, I., Demirtas, M., Çolak, I.. "Application of One-Axes sun Tracking System". Energy Conversion and Management. 2009. Page 2710.
- [28] Vorobiev, P. Yu, Jesús Gonzalez-Hernandez, and Yuri V. Vorobiev. "Optimization of the solar energy collection in tracking and non-tracking photovoltaic solar

References

system." (ICEEE). 1st International Conference on Electrical and Electronics Engineering, 2004.. IEEE, 2004.